The Thesis Committee for Baylie Nicole Burke
Certifies that this is the approved version of the following thesis:

Monomer Screening for Sequence Defined Polymerization in a Genetically Modified Ribosome

APPROVED BY
SUPERVISING COMMITTEE:

Eric V. Anslyn, Supervisor

Simon Humphrey

Monomer Screening for Sequence Defined Polymerization in a Genetically Modified Ribosome

by

Baylie Nicole Burke

Thesis

Presented to the Faculty of the Graduate School of

The University of Texas at Austin

in Partial Fulfillment

of the Requirements

for the Degree of

Master of Arts

The University of Texas at Austin

May 2018

Acknowledgements

First and foremost, I would like to thank my advisor Eric Anslyn for his undying kindness and enthusiasm for research. Whenever I was frustrated with my project not working as anticipated, he was understanding and encouraging, providing me with the drive and inspiration to continue forward.

I would especially like to thank members of the Anslyn group, in particular Rogelio Escamilla, for helping me through my project, especially when I felt completely stuck and didn't know where to go next, even though he had much better things to do. I would also like to thank my great friends, Caroline Hinson, Leyah Schwartz, Maggie Meadows, Liz Gratton, Sarah Moor, and Stephanie Valenzuela for the awesome girls' nights and workout sessions I will always cherish. I'd like to thank all of "loud side" of the Anslyn group, Brenden Herrera, Logan Bachman, Sam Dahlhauser, Rogelio Escamilla, Igor Kolesnichenko, Chris White (honorary loud side member), and even Pedro Metola, as they have helped answer all of my questions, and their goofy antics have made the long days fly by. I wish all of the Anslyn and Iverson group, past and present, all the best in the future!

Finally, I would also like to thank my husband, Adam, and my family for their undying support and love. They saw me through thick and thin, and I will be forever grateful. Thank you, Adam, Luna, Zara, and even Andrew and Chomper, for creating a home that I love so much, and for providing the support I needed!

Monomer Screening for Sequence Defined Polymerization in a Genetically Modified Ribosome

Baylie Nicole Burke, M.A.

The University of Texas at Austin, 2018

Supervisor: Eric V. Anslyn

Sequence defined polymers, or polymers of a pre-determined length and sequence, are the "Holy Grail" of polymer synthesis. As the physical properties of polymers are highly dependent upon their chemical composition, the wide range of potential applications for sequence defined polymers has yet to be explored. After millions of years of evolution, the ribosome has become a highly efficient polymerization catalyst. In this project, we will work to capitalize on this efficiency to work to create unnatural sequence defined polymers in a genetically modified ribosome. Collaborators in the Jewett group are currently genetically modifying the ribosomal active site to widen the library of chemistries the ribosome is able to catalyze, while we are exploring the chemistries of monomers that could be polymerized by a genetically modified ribosome. This thesis will first identify monomers capable of polymerization under the restricted conditions set by the ribosome, followed by synthesis of promising monomers, and finally taking steps towards loading the synthesized monomers onto tRNA.

Table of Contents

List of Figures ix

PART 1: MONOMER TEST SCHEMES AND SYNTHESIS 1

Chapter 1: Introduction and Background 1

Chapter 2: Results and Discussion 3

2.1 Test Reactions 3

2.1.1 Scheme 1: Carbazate 3

2.1.2 Scheme 2: Hydrazinoacetate 4

2.1.3 Scheme 3: 4-Aminomethyl Phthalate 4

2.1.4 Scheme 4: 4-Hydrazino Cinnamate 5

2.1.5 Scheme 5: 4-Hydrazino Phenylpropiolate 5

2.1.6 Scheme 6: 4-Hydrazino Benzoylacetate 6

2.1.7 Scheme 7: 1-Formyl-2-Amino Phenylcyanoacetate 6

2.1.8 Scheme 8: 1-Formyl-2-Amino Triphenylphosphine Phenylacetate 7

2.1.9 Scheme 9: 1-Formyl-2-Amino Bromophenylacetate 7

2.2 Scheme 6 Monomer Synthesis 8

2.2.1 Plan 1 8

2.2.2 Plan 2 10

Chapter 3: Conclusion and Future Work 13

3.1 New Test Reaction 13

3.2 Scheme 3 Monomer Synthesis 13

Chapter 4: Experimental 14

4.1 Materials and Methods 14

4.2 Test Reactions 14
4.2.1 General Screening Procedure 14
4.2.2 Scheme 3 Test Reaction 15
4.2.3 Scheme 4 Test Reaction 18
4.2.4 Scheme 5 Test Reaction 19
4.2.5 Scheme 6 Test Reaction 23
4.2.6 Scheme 9 Test Reaction 27
4.3 Monomer Synthesis 29
4.3.1 Plan 1 29
4.3.1.1 Claisen Reaction 29
4.3.1.2 Nitro Reduction 32
4.3.1.3 Diazotization 35
4.3.1.4 Test Diazotization 36
4.3.2 Plan 2 36
4.3.2.1 Fischer Esterification 36
4.3.2.2 Tri-Boc Protection 39
4.3.2.3 Claisen Reaction 42
4.3.2.4 Boc-Deprotection 49
Chapter 5: References for Part 1 53
PART 2: PREPARATION FOR PDCPA CHARGING 55
Chapter 6: Introduction and Background 55
Chapter 7: Results and Discussion 57
7.1 NVOC-Cl Synthesis 57

7.2 pdCpA Synthesis....58
7.2.1 Schultz's Method....58
7.2.2 Automated DNA Synthesizer....59
7.2.3 Manual DNA Synthesizer Method....60
Chapter 8: Conclusions and Future Work....61
Chapter 9: Experimental....63
9.1 Materials and Methods....63
9.2 NVOC-Cl Synthesis....63
9.3 pdCpA Synthesis....65
9.3.1 Automated DNA Synthesizer Method....65
9.3.2 Manual DNA Synthesizer Method....66
Chapter 10: References for Part 2....70
Bibliography....72

List of Figures

Figure 2.1: Scheme 1 test reaction and accompanying monomer charged to tRNA. 3

Figure 2.2: Scheme 2 test reaction and accompanying monomer charged to tRNA. 4

Figure 2.3: Scheme 3 test reaction and accompanying monomer charged to tRNA. 4

Figure 2.4: Scheme 4 test reaction and accompanying monomer charged to tRNA. 5

Figure 2.5: Scheme 5 test reaction and accompanying monomer charged to tRNA. 5

Figure 2.6: Scheme 6 test reaction and accompanying monomer charged to tRNA. 6

Figure 2.7: Scheme 7 test reaction and accompanying monomer charged to tRNA. 6

Figure 2.8: Scheme 8 test reaction and accompanying monomer charged to tRNA. 7

Figure 2.9: Scheme 9 test reaction and accompanying monomer charged to tRNA. 7

Figure 2.10: Scheme 6 monomer synthesis plan 1. 8

Figure 2.11: Test Diazotization of 11.. 9

Figure 2.12: Scheme 6 monomer synthesis plan 2.. 10

Figure 2.13: Products observed during the Claisen Reaction of 15.....11

Figure 3.1: New test reaction based on Scheme 10 developed for investigation.. 13

Figure 3.2: Monomer synthesis for Scheme 3 test reaction......13

Figure 4.1: ^{1}H-NMR (400 MHz) in CD_3OD of 3.. 16

Figure 4.2: ^{13}C-NMR (500 MHz) in $CDCl_3$ of 3. 17

Figure 4.3: ^{1}H-NMR (400 MHz) in CD_3OD of Scheme 4 test reaction... 18

Figure 4.4: ^{1}H-NMR (500 MHz) in $CDCl_3$ of 5. 20

Figure 4.5: ^{1}H-NMR (500MHz) in $(CD_3)_2SO$ of 5. 21

Figure 4.6: ^{13}C-NMR (500 MHz) in $CDCl_3$ of 5.. 22

Figure 4.7: High Resolution Mass Spectrum (ESI positive mode) of 5.. 23

Figure 4.8: ^{1}H-NMR (500 MHz) in $CDCl_3$ of 6. 24

Figure 4.9: ^{13}C-NMR (500 MHz) in $CDCl_3$ of 6.. 25
Figure 4.10: High Resolution Mass Spectrum (ESI positive mode) of 6.. 26
Figure 4.11: High Resolution Mass Spectrum (ESI negative mode) of 6.. 26
Figure 4.12: LC/MS data of Scheme 9. LC traces: at 254 nm, 214 nm, and 280 nm (frames 1-3). Mass detection: ESI/APCI positive ionization (frame 4), ESI/APCI negative ionization (frame 5).. 27
Figure 4.13: ESI/APCI positive ionization mass spectrum from 8.2 to 8.6 min.. 28
Figure 4.14: ESI/APCI negative ionization mass spectrum from 8.3 to 8.6 min. 28
Figure 4.15: ^{1}H-NMR (500 MHz) in $CDCl_3$ of 10.. 30
Figure 4.16: ^{13}C-NMR (500 MHz) in $CDCl_3$ of 10. 31
Figure 4.17: High Resolution Mass Spectrum (ESI positive mode) of 10.. 32
Figure 4.18: ^{1}H-NMR (500 MHz) in $CDCl_3$ of 11. 33
Figure 4.19: ^{13}C-NMR (500 MHz) $CDCl_3$ of 11. 34
Figure 4.20: High Resolution Mass Spectrum (ESI positive mode) of 11.. 35
Figure 4.21: ^{1}H-NMR (400 MHz) in CD_3OD of 14.. 37
Figure 4.22: LC/MS of 14. LC traces: at 254 nm, 214 nm, and 280 nm (frames 1-3). Mass detection: ESI/APCI positive ionization (frame 4), ESI/APCI negative ionization (frame 5).. 38
Figure 4.23: ESI/APCI positive ionization mass spectrum from 2.8 to 3.1 min of 14.. 38
Figure 4.24: ^{1}H-NMR (500 MHz) in $CDCl_3$ of 15.. 40
Figure 4.25: ^{13}C-NMR (500 MHz) in $CDCl_3$ of 15.. 41
Figure 4.26: High Resolution Mass Spectrum (ESI positive mode) of 15.. 42
Figure 4.27: ^{1}H-NMR (500 MHz) in $CDCl_3$ of 18.. 44
Figure 4.28: ^{13}C-NMR (500 MHz) in $CDCl_3$ of 18.. 45
Figure 4.29: High Resolution Mass Spectrum (ESI positive mode) of 18.. 46

Figure 4.30: 3D LC trace of Claisen Reaction of 15. 46
Figure 4.31: ESI/APCI positive ionization mass spectrum from 12.6 to 12.9 of 15. $[M+Na]^+$ expected 503. $[2M+Na]^+$ expected 983.. 47
Figure 4.32: ESI/APCI positive ionization mass spectrum from 11.8 to 12.1 of 16. $[M+Na]^+$ expected 545. $[2M+Na]^+$ expected 1067.. 47
Figure 4.33: ESI/APCI positive ionization mass spectrum from 11.0 to 11.3 of 17. $[M+Na]^+$ expected 403. $[2M+Na]^+$ expected 783.. 48
Figure 4.34: ESI/APCI positive ionization mass spectrum from 10.3 to 10.5 of 18. $[M+Na]^+$ expeted 445.. 48
Figure 4.35: High Resolution Mass Spectrum (ESI positive mode) of M6.. 50
Figure 4.36: Hypothesized M6 dimer moiety... 51
Figure 4.37: LC/MS data of M6 and dimer after lyophilization. LC traces: at 254 nm, 214 nm, and 280 nm (frames 1-3). Mass detection: ESI/APCI positive ionization (frame 4), ESI/APCI negative ionization (frame 5).... 51
Figure 4.38: ESI/APCI negative ionization mass spectrum from 7.0 to 7.3 of M6 dimer. $[M-H]^-$ expected 379. 52
Figure 6.1: Ribosome with the small and large subunits, mRNA, tRNA, and the amino acids in the PTC site. 55
Figure 7.1: NVOC-Cl synthesis.. 57
Figure 7.2: Schultz's manual synthesis.. 58
Figure 7.3: pdCpA synthesis by DNA Synthesizer.. 59
Figure 8.1: Scheme 7 monomer charging onto tRNA via pdCpA.. 61
Figure 8.2: Scheme 3, 6, and 7 monomers with possible positions of variability.. 62
Figure 9.1: ^{1}H-NMR (400 MHz) $CDCl_3$ of 20.. 64
Figure 9.2: ^{1}H-NMR (400 MHz) $CDCl_3$ of NVOC-Cl.. 65

Figure 9.3: High Resolution Mass Spectrum (ESI positive mode) of 20.. 66
Figure 9.4: High Resolution Mass Spectrum (ESI negative mode) of 20.. 69

PART 1: MONOMER TEST SCHEMES

Chapter 1: Introduction and Background

Polymers have an amazingly wide range of applications in today's world for everyday uses for cars and clothing, to specifically engineered applications like Kevlar for bullet-proof vests. Molecular attributes of polymers such as molecular weight distribution, tacticity (stereochemistry), and arrangement of co-polymerization (block/branched/random) are directly related to their chemical composition and determine the polymer's physical characteristics such as physical strength, permeability, and conductance. Due to this correlation, methods to regulate the chemical structure of polymers are of high interest. Current methods of synthesizing polymers include mixed-pot reactions, where reagents are added simultaneously producing a wide range of polymers, and batch polymers where reagents are added sequentially, which allows for some control on block co-polymerization but still produces a wide molecular weight distribution. Alternatively, a catalyst can be utilized to create more regular, stereospecific polymers, but even this method produces a variety of molecular weights. Sequence defined polymers, or polymers made of a pre-defined length and sequence, are considered the "Holy Grail" of polymer synthesis and have not yet been achieved.

In nature, sequence defined polymers are regularly synthesized based upon a provided mRNA template by the ribosome, which can be thought of as a polymerization catalyst. The reaction speed and error checking achieved by the ribosome make it an ideal candidate for creating sequence defined polymers on a large scale. In an attempt to capitalize on this highly efficient catalyst, the design and testing of possible non-amino-acid monomers that could be catalyzed by a ribosome will be investigated. Additionally, the genetic modification of the ribosomal active site will be under investigation by

collaborators in the Jewett group in order to polymerize a wider range of unnatural monomers.

In-vivo, ribosomes have only been observed to catalyze the creation of polyamides, though the natural ribosome has also been shown to catalyze the formation of polyesters in-vitro.[1-3] Before attempting to use the ribosome to synthesize a non-amide-backbone polymer, an appropriate monomer must be found. The monomer must be soluble in water and unreactive under standard physiological conditions (pH 7, 20˚C) to prevent side reactions occurring outside the ribosome. Additionally, the monomer must be small enough to fit in the active site of the ribosome, and the newly formed polymer must fit through the peptide exit tunnel, which has a diameter of 10 to 20 Å.[4] Finally, the ribosome must be able to tolerate the polymerization conditions, that is to say the reaction conditions for polymerization must mild (not too acidic/basic, and not above 100˚C).

The structure of the amino acid consists of an ester to attach to tRNA, the shuttle that brings amino acids into the ribosome, and a nucleophilic group, a free amine, that can cleave the ester group of another amino acid to separate the growing peptide from the tRNA. The resulting peptide will now become the new electrophilic ester for attack by a new incoming amino acid. To utilize the ribosome for polymerization, our designed monomers must also contain these two functionalities, an ester group and a nucleophilic group.

To find a monomer that matches all of these criteria, test reactions first must be screened outside of the ribosome to determine the conditions required for reaction. The monomers to be tested will be modeled after amino acids and will become more variable in structure as testing continues. As more complicated chemistries are applied to this process, more genetic modification of the ribosome may need to occur.

Chapter 2: Results and Discussion

2.1 TEST REACTIONS

To determine monomers likely to be polymerized in a genetically modified ribosome, test reactions were performed to determine the reaction conditions required for polymerization of various monomer candidates. Nine schemes were designed and tested under a series of conditions, beginning with equimolar starting material at room temperature, followed by the addition of base, and subsequent gradual heating. Reactions were monitored by ^{1}H-NMR and TLC for the appearance of product formation. Upon observed product formation, the reaction was scaled up to isolate and further characterize the product(s) formed. If the desired product was indeed formed under the required conditions set by the ribosome, monomer synthesis would begin.

2.1.1 Scheme 1: Carbazate

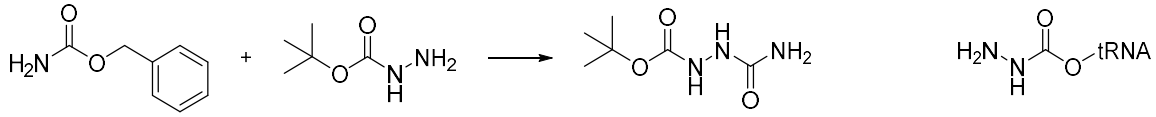

1 **M1**

Figure 2.1: Scheme 1 test reaction and accompanying monomer charged to tRNA.

After a series of increasingly rigorous conditions, the last of which consisted of 1.1 equivalents potassium phosphate tribasic and heating at 75˚C, the only product observed was the trans-esterification product. Because this scheme did not form the desired product under the required conditions set by the ribosome, it was concluded that this monomer was not likely to be reactive enough to be catalyzed by a ribosome.

2.1.2 Scheme 2: Hydrazinoacetate

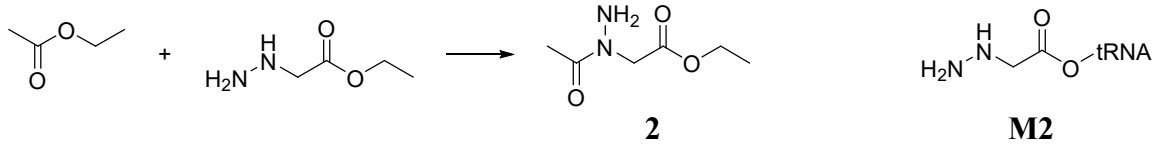

Figure 2.2: Scheme 2 test reaction and accompanying monomer charged to tRNA.

After reaction with 1.1 equivalents potassium phosphate, ethyl hydrazinoacetate HCl, and excess ethyl acetate at 75˚C. No desired amide bond formation was observed, and it was determined would not be favorable for polymerization in a ribosome.

2.1.3 Scheme 3: 4-Aminomethyl Phthalate

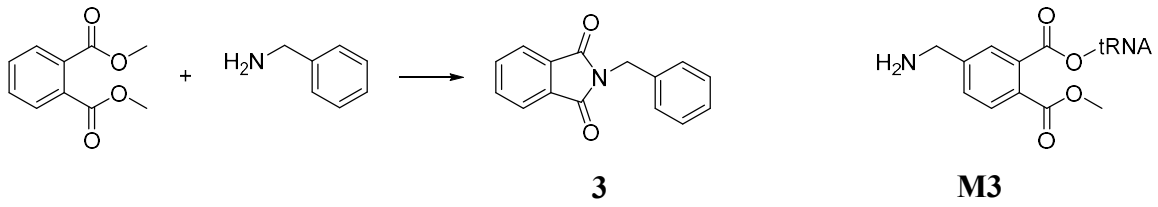

Figure 2.3: Scheme 3 test reaction and accompanying monomer charged to tRNA.

Imide bond formation is utilized in several commercially available polymers, including Kapton and Matrimid®, which with their high-heat and chemical resistance, typically are used for insulation, gas filters, and flexible tubing.[5] Imide bond formation is ideal for ribosome catalysis because of its simplicity and close relation to natural peptide bond formation.

The reaction was performed neat in triethylamine at 100˚C. **3** was successfully isolated and characterized by ^{1}H-NMR and ^{13}C-NMR. Out of concern for the ability of the ribosome to remain functional at the high temperature of 100˚C, a temperature study monitored by ^{1}H-NMR in CD_3OD was performed, which showed conversion of 50% at 80˚C and 45% at 75˚C over 48 hours and confirmed product formation under aqueous

conditions. The synthesis of the designed monomer will continue forward under the hypothesis that the catalytic ability of the ribosome may help overcome the required high temperatures for reaction.

2.1.4 Scheme 4: 4-Hydrazino Cinnamate

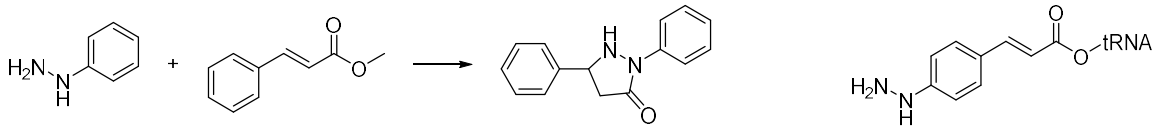

Figure 2.**4**: Scheme 4 test reaction and accompanying monomer charged to tRNA.

The proposed mechanism proceeds 1,4- Michael addition of phenyl hydrazine, followed by cyclization and displacement of the ester. However, upon reaction with sodium acetate at 70˚C, the only formed product was the amide product, without the Michael addition. Upon further consideration, it was realized the cyclization from the amide product is disfavored under Baldwin's rule.[6] Therefore, it was determined that this reaction would not go forward as planned, and instead we pursued the alkyne, which was predicted to cyclize.

2.1.5 Scheme 5: 4-Hydrazino Phenylpropiolate

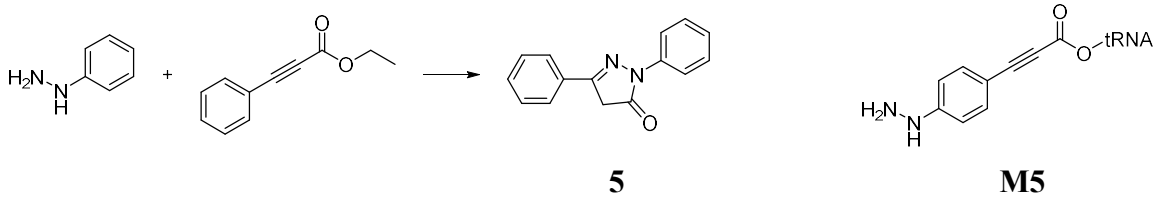

Figure 2.5: Scheme 5 test reaction and accompanying monomer charged to tRNA.

The reaction of phenyl hydrazine with ethyl phenylpropiolate at 80˚C with calcium carbonate formed the desired product, **5**. The product was isolated and purified by

CombiFlash and characterized by ^{1}H-NMR, ^{13}C-NMR, and HRMS. This scheme will continue with monomer synthesis, as it reacts well under the required conditions.

2.1.6 Scheme 6: 4-Hydrazino Benzoylacetate

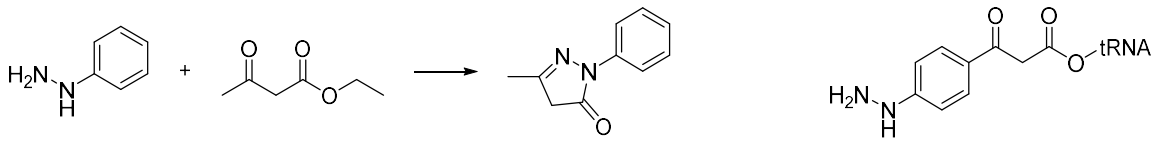

Figure 2.6: Scheme 6 test reaction and accompanying monomer charged to tRNA.

The reaction of phenyl hydrazine, ethyl acetoacetate, and sodium acetate at 75˚C was performed following a protocol provided by Kudirka, et al.[7] The major product was isolated, purified, and characterized by ^{1}H-NMR, ^{13}C-NMR, and HRMS to show the formation of the desired product, **7**. This scheme has been continued onto monomer synthesis for attachment onto tRNA.

2.1.7 Scheme 7: 1-Formyl-2-Amino Phenylcyanoacetate

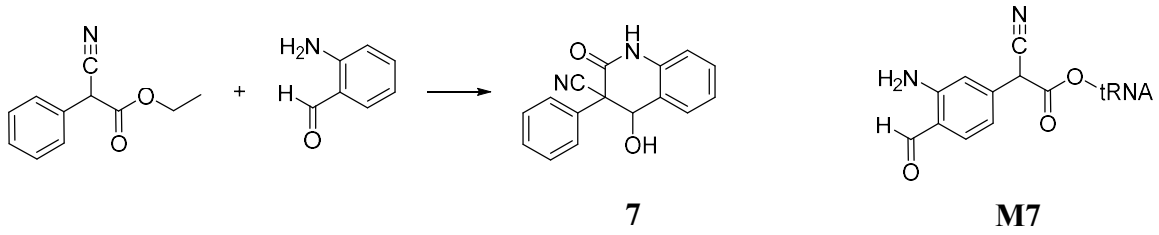

Figure 2.7: Scheme 7 test reaction and accompanying monomer charged to tRNA.

After a series of test reactions, the formation of a variety of products was observed. 2-amino benzaldehyde was observed to form homodimer and homotrimer moieties. Upon LC/MS testing of the starting material, these moieties were observed in low concentration, which increased upon addition of temperature and base. Another product's structure was not able to be determined; however, during a pH titration study of ethyl

phenylcyanoacetate, this product was observed. At this time, it was determined that ethyl phenylcyanoacetate preferentially reacts with itself over reacting with amino benzaldehyde, so this reaction was reworked with different substituents in the alpha-position.

2.1.8 Scheme 8: 1-Formyl-2-Amino Triphenylphosphine Phenylacetate

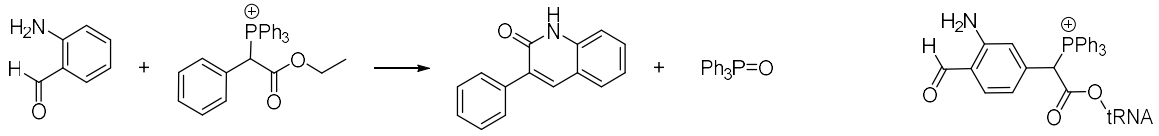

8 **M8**

Figure 2.8: Scheme 8 test reaction and accompanying monomer charged to tRNA.

Colleagues in the Moore group synthesized ethyl-α-triphenylphosphine phenylacetate, which was subjected to base and thurough heating. No product formation was observed by LC/MS or ^{1}H-NMR, except for the previously observed formation of homodimer and homotrimer 2-amino benzaldehyde. It was determined that the triphenylphoshine moiety was also not reactive enough to form the desired product.

2.1.9 Scheme 9: 1-Formyl-2-Amino Bromophenylacetate

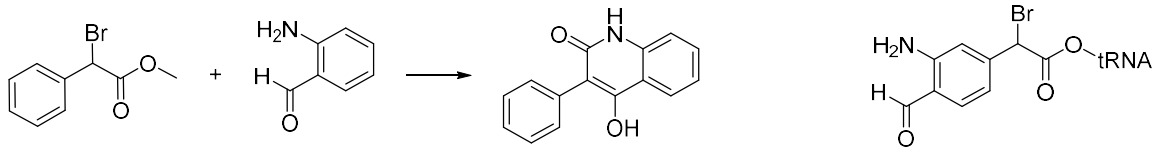

9 **M9**

Figure 2.9: Scheme 9 test reaction and accompanying monomer charged to tRNA.

Upon reaction of methyl a-bromophenylacetate with benzoic acid at 60˚C with potassium phosphate tribasic, formation of a single product was observed. After

purification and characterization by LC/MS and ^{1}H-NMR, it was determined that the amine performed nucleophilic attack displacing the bromine instead of the desired ester. The result of which prevents cyclization to the desired product. Upon further consideration, this scheme has been reconsidered, and a new scheme, **Figure 3.1**, will be tested next.

2.2 SCHEME 6 MONOMER SYNTHESIS

2.2.1 Plan 1

Based upon the results of the test schemes, Scheme 3, Scheme 5, and Scheme 6 were determined to react under the desired conditions. Scheme 6 was selected as the most likely to be successfully polymerized in a ribosome due to its high yield under mild conditions. An original synthesis plan (**Figure 2.10**) was created and tested.

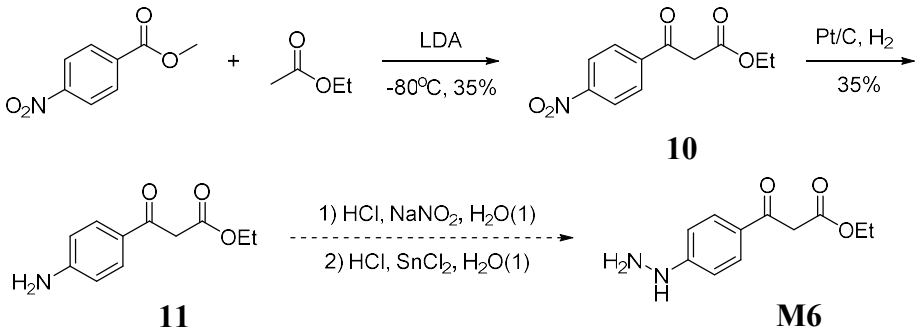

Figure 2.10: Scheme 6 monomer synthesis plan 1.

Following work by Rostovskii, et al., the ethyl acetate enolate was formed in LDA, followed by addition of 4-nitrobenzoate.[8] The reaction was quenched with 20% HCl and extracted to produce **10** with few side products. By ^{1}H-NMR and LC/MS, both the keto and enol form of the compound were observed in solution and were only able to be separated by recrystallization.

Upon initial attempt to perform nitro reduction on **10**, a large amount of undesired side product formation was observed, the main of which was determined to be the reduced ketone product. Thus, a series of test reduction conditions were performed including: 10% Pd and Pt on activated carbon, Sn(II)Cl·2H_2O, and Iron powder.[9-14] It was determined that 10% Pt on activated carbon under bubbling H_2(g) for 30 minutes produced approximately 80% **11**, but 20% still formed the alcohol bi-product. Pure **11** was isolated by HPLC, and characterized by ^{1}H-NMR, ^{13}C-NMR, and HRMS.

The third step of the monomer synthesis was performed following the procedure outlined by Kuznetsova, et al.[9] Upon analysis by LC/MS, the reaction was not forming **M6**, and did not leave **11** intact. In an effort to determine whether the diazotization or the reduction was forming undesired side products, the test diazotization outlined in **Figure 2.11** was performed on **11**. This test diazotization has been well studied in our group and has been shown to work on a variety of amine-containing compounds with consistently high yield and few side products.

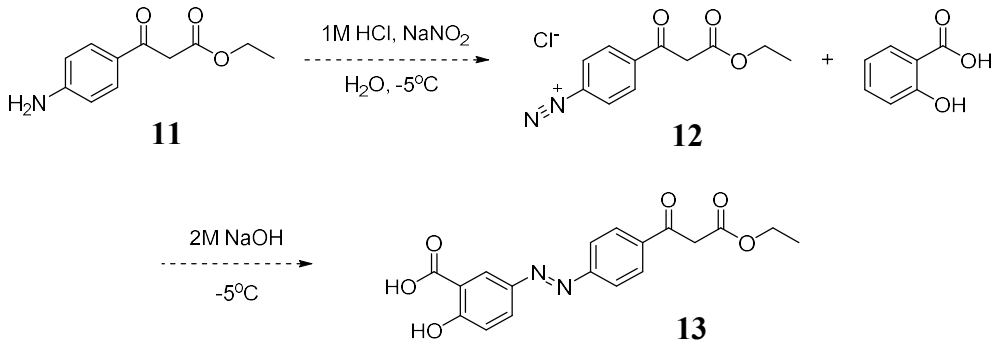

Figure 2.11: Test Diazotization of **11**.

Firstly, the diazonium salt is created, followed by immediate addition to the salicylic acid, while basic conditions are maintained, and characterization by LC/MS performed at both steps in the process. An undesired product formation was observed after

the diazotization step with no change after the coupling step. Based upon the LC/MS data, it was hypothesized that once **12** is formed, it immediately reacted with another of the β-keto ester compounds at the enol position and did not wait for the addition of salicylic acid. It was concluded this was likely the cause of failure of both diazotization reactions.

In an attempt to both increase the yield of the reduction step and to get the diazotization/reduction step to work, protection of the ketone of **10** with ethylene glycol was investigated following various protocols.[15-16] In all cases, only unreacted **10** was observed. It was hypothesized that because the enol form of **10** is the predominant form, protection of the ketone would not be favored. Based on these results, it was determined that the synthetic route needed to be reevaluated.

2.2.2 Plan 2

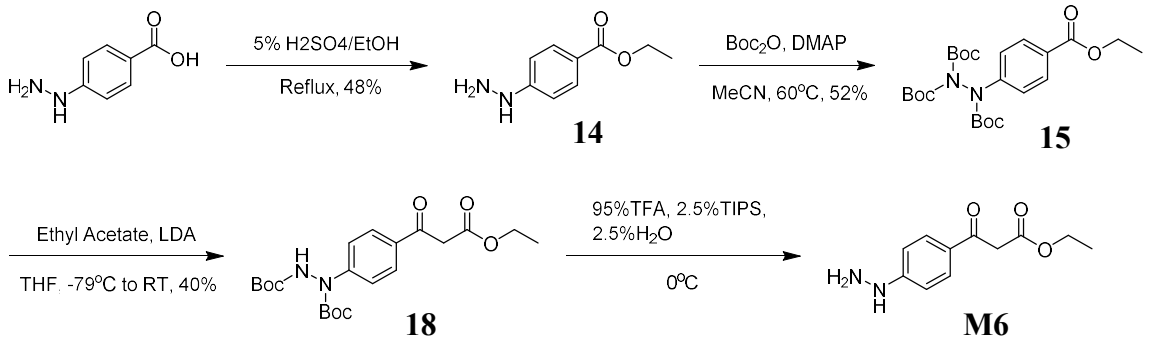

Figure 2.12: Scheme 6 monomer synthesis plan 2.

Figure 2.12 demonstrates the new monomer synthesis plan, with the intention of performing the Claisen reaction last, as it had already been shown to work well. Firstly, Fischer Esterification was performed with 5% H_2SO_4/EtOH at reflux followed by quenching, extraction, and concentration to provide **14** as a pure yellow solid, which was characterized by LC/MS.

Boc protection of **14** was accomplished with excess Boc anhydride, catalytic amounts of DMAP, and heating for several hours.[17] Purification of crude product by CombiFlash produced **15** as a viscous orange liquid, confirmed by ^{1}H-NMR, ^{13}C-NMR, and HRMS.

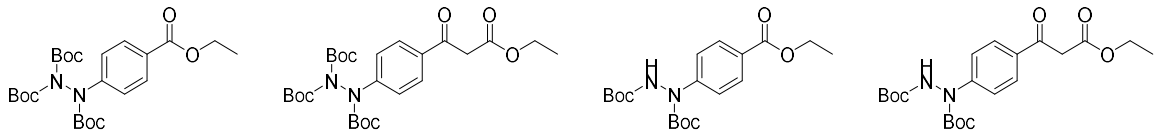

15 **16** **17** **18**

Figure 2.13: Products observed during the Claisen Reaction of **15**.

The Claisen reaction was performed following the same procedure as outlined previously, but when the reaction was kept at -80˚C, only 10% conversion of **15** to **16** was observed. The reaction was then run again with gentle warming to room temperature overnight, where production of **16**, **17**, and **18** were observed, and at completion 45% conversion to **18**, with 55% conversion to **17** was observed. CombiFlash provided isolation of **17**, which could then undergo the Boc reaction again, and pure **18** for characterization by ^{1}H-NMR, ^{13}C-NMR, and HRMS.

Finally, deprotection of **18** was attempted through a series of deprotection procedures. From characterization by LC/MS, **18**, mono-Boc, and **M6** were observed, but also a major, undesired side product. Upon work-up, any **M6** that formed would readily decompose to this side product. After a vigorous series of sample deprotections, the reaction condition that provided the most **M6**, and minimized side product formation was a TFA/TIPS/H_2O cocktail reacted at -5˚C for 2 to 3 hours. The reaction was monitored by injectable mass spec, and dried by blowing N_2(g) over the solution while carefully maintaining -5˚C. The compound was then dissolved in dH_2O at 0˚C and immediately

purified by CombiFlash. Analysis of the fractions collected from the CombiFlash showed pure product (by injectable mass spec). Fractions containing **M6** were lyophilized producing a very fine yellow powder, which was then characterized by injectable mass spec and LC/MS. The lyophilized product contained of a small amount of **M6**, but mostly consisted of a new side product that appeared to be a polymer form. At this point, it was determined that the deprotected monomer would be too reactive to charge to pdCpA, so investigation will continue with different protecting groups (possibly NVOC-Cl) during monomer synthesis that could be cleaved in-situ for polymerization.

Chapter 3: Conclusions and Future Work

3.1 New Test Reaction

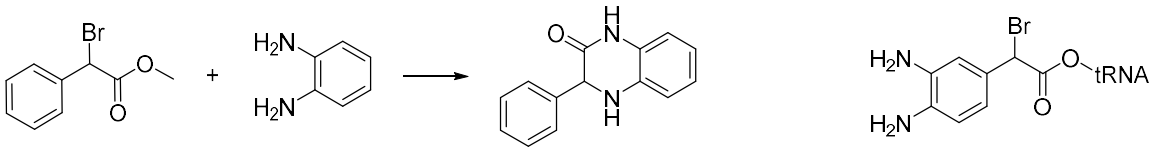

Figure 3.1: New test reaction based on Scheme 10 developed for investigation.

Similar to Scheme 10, this new test reaction was designed. After nucleophilic attack to displace the bromine, there is still a free amine to attack the ester to form a cyclic product, which would consist of one amide and one secondary amine. It is hopeful this reaction could occur in the desired conditions based upon the results of the previous test reactions.

3.2 Scheme 3 Monomer Synthesis

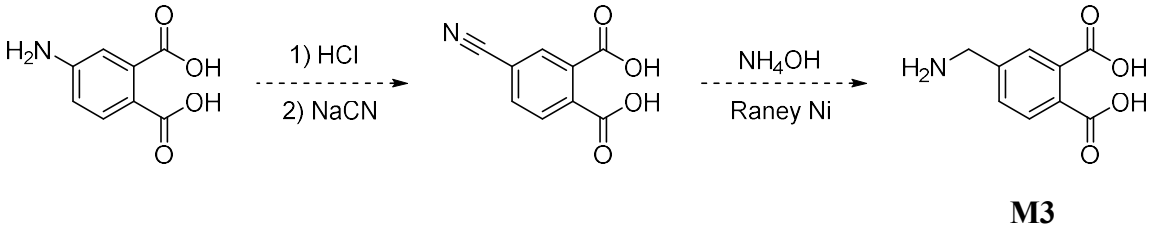

M3

Figure 3.2: Monomer synthesis for Scheme 3 test reaction.

The next monomer to be synthesized for charging tRNA will be for Scheme 3 by combining an allylic amine with a phthalate onto one ring. Firstly, the amine will be displaced by potassium cyanide, followed by reduction of the nitrile.[18-19]

Chapter 4: Experimental

4.1 Materials And Methods

Ethyl α-triphenylphosphine phenylacetate was synthesized by the Moore group, and sent to us for testing. All other chemicals were of reagent grade and used as purchased without further purification. LC/MS spectra were obtained on an Agilent Technologies 6120 Single Quadrupole LC/MS spectrometer which utilized a 5-95% MeOH/H_2O gradient over 12 minutes, with atmospheric-pressure chemical ionization in both positive and negative mode. ^{1}H-NMR (400 MHz) were acquired with an Agilent 400 MHz. ^{1}H-NMR (500 MHz) and ^{13}C-NMR were acquired with a Bruker AVANCE III 500 MHz.

4.2 Test reactions

4.2.1 General Screening Procedure

Each test reaction began with an ^{1}H-NMR and TLC study for the presence of any new products, at which time characterization by LC/MS was performed. 0.2 mmol of each starting material were separately characterized by ^{1}H-NMR in 1.0 mL CD_3OD or if insoluble, a mixture of D_2O/CD_3OD. Then 0.2 mmol of one compound was added to the other compound dissolved in the deuterated solvent, and the mixture was allowed to stir at room temperature overnight and followed by characterized by ^{1}H-NMR. If no product had formed, 1.1 equivalents of base (typically potassium phosphate tribasic, as it does not show on ^{1}H-NMR) was added to solution, and again stirred at room temperature overnight and characterized by ^{1}H-NMR. Finally, heating began at sequentially higher temperatures overnight (45˚C, 60˚C, 75˚C), followed by ^{1}H-NMR Characterization. At this time, LC/MS screening would occur, and if no new product formation had occurred, the scheme would

be determined not to work under desired conditions, and investigation into the scheme would conclude.

If at any point in this ^{1}H-NMR study, new peaks were observed, the solution was characterized by LC/MS. If the formed product matched the expected molecular weight of the desired product, the reaction was scaled up for product isolation by column chromatography. The pure product then would be characterized by ^{1}H-NMR, ^{13}C-NMR, and LC/MS to identify the formed product.

4.2.2 Scheme 3 Test Reaction

Dimethyl phthalate (0.640 mmol, 1.0 eq.), benzyl amine (0.613 mmol, 1.0 eq.), and triethylamine (0.645 mmol, 1.0 eq.) were added to a vial without solvent and heated at 103˚C for at least eight hours until no starting material was observed by TLC (dissolved in methanol, run in 5:1 hexanes:ethyl acetate). After cooling to room temperature, solution was dissolved in 1:1 methanol:dichloromethane and purified by column chromatography (5:1 hexanes:ethyl acetate). Fractions containing product were combined and concentrated under reduced pressure to produce a white puffy solid, **3**, which was characterized by ^{1}H-NMR and ^{13}C-NMR in CD_3OD. (0.071 g, 48.9% yield).

(**Figure 4.1**) 1H NMR (400 MHz, Methanol-d4) δ 7.90 – 7.78 (m, 4H), 7.38 – 7.22 (m, 5H), 4.83 (s, 2H), 2.16 (s, 1H). (**Figure 4.2**) 13C NMR (126 MHz, Chloroform-d) δ 168.18, 136.50, 134.11, 132.27, 128.81, 128.75, 127.96, 123.48, 41.75.

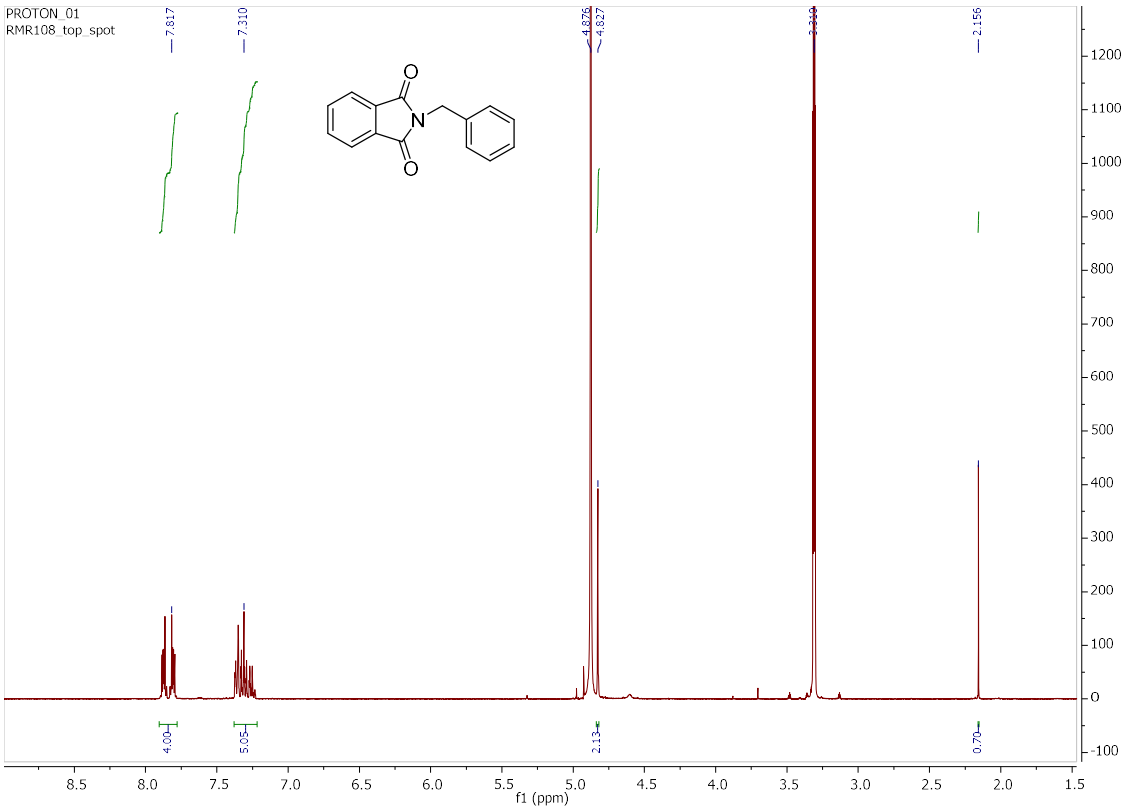

Figure 4.1: ^{1}H-NMR (400 MHz) in CD_3OD of **3**.

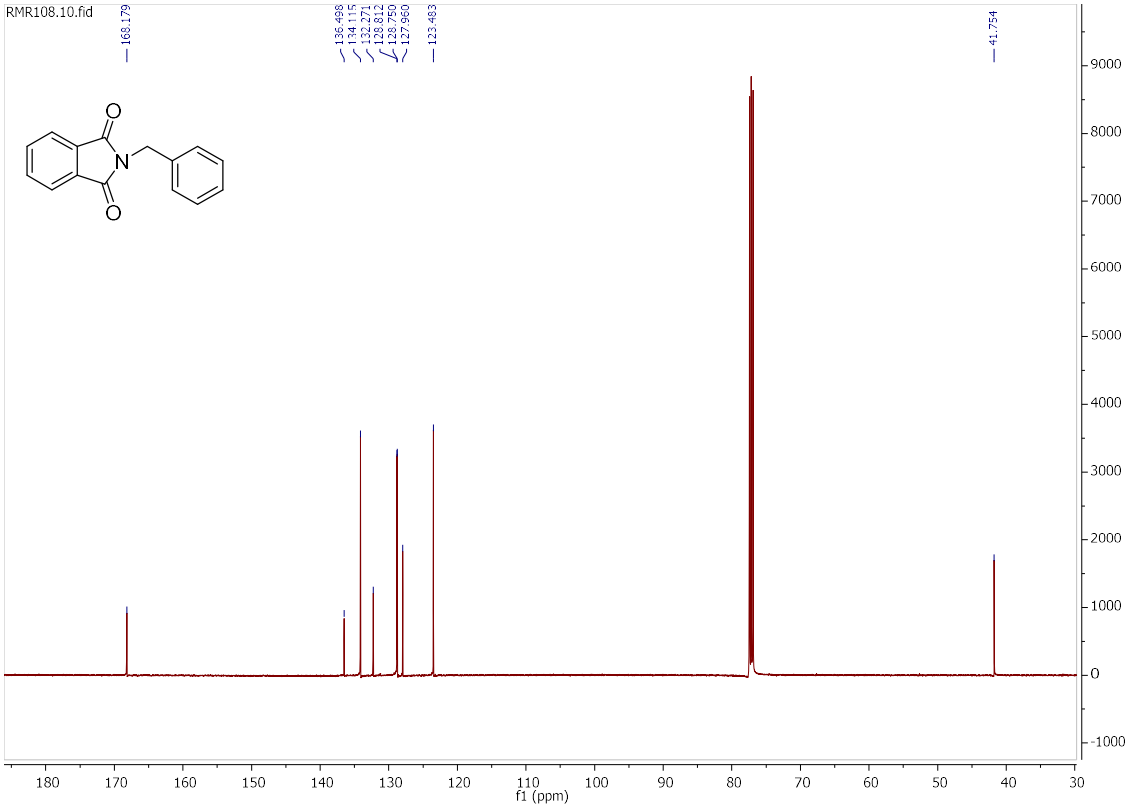

Figure 4.2: ^{13}C-NMR (500 MHz) in $CDCl_3$ of **3**.

Additionally, a ^{1}H-NMR control study was carried out to determine the percent conversion to **3** at varying temperatures. Aromatic starting material peaks were integrated in reference to desired **3** aromatic peaks, in which there was no overlap, so a percent conversion could be calculated. At 60˚C, no product formation was observed; at 75˚C, 20% conversion was observed at 24 hours, and 45% conversion was observed at 48 hours; at 80˚C conversions of 40% and 50% were observed, respectively; at 90˚C, 85% conversion was observed after 24 hours. 60˚C and 90˚C were not continued in the 48 hour tests due to faulty hot plates.

4.2.3 Scheme 4 Test Reaction

Methyl *trans*-cinnamate (1.233 mmol, 1.0 eq.) was dissolved in 4.0 mL methanol, followed by addition of phenyl hydrazine (1.220 mmol, 1.0 eq.) and sodium acetate (1.220 mmol, 1.0 eq.). The solution was heated at 70˚C over the weekend until new product was observed by TLC. The solution was cooled to room temperature, then purified by column chromatography (3:1 ethyl acetate:hexanes). Fractions were collected, concentrated under reduced pressure, and characterized by ^{1}H-NMR and LC/MS (compound does not ionize in mass spec) to show the formation of the amide bond formation without cyclization.

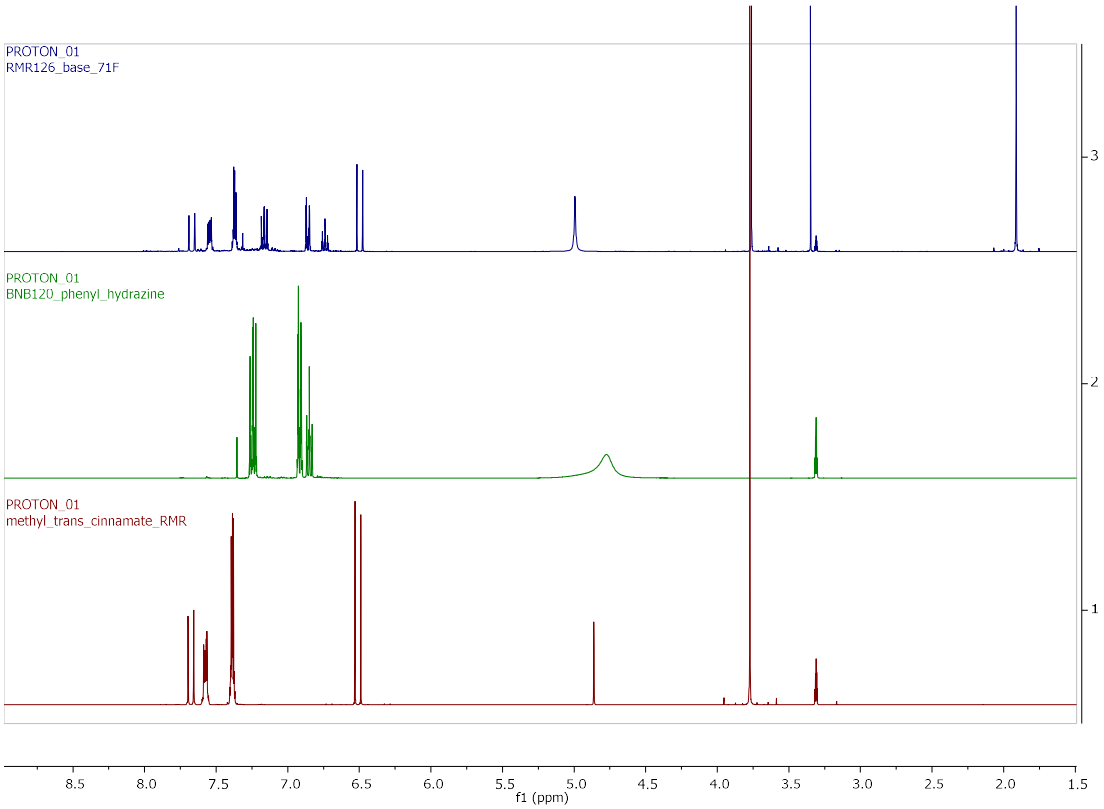

Figure 4.3: ^{1}H-NMR (400 MHz) in CD_3OD of Scheme 4 test reaction.

4.2.4 Scheme 5 Test Reaction

Ethyl phenylpropiolate (0.999 mmol, 1.0 eq), phenyl hydrazine (1.002 mmol, 1.0 eq.), and calcium carbonate (1.199 mmol, 1.2 eq.) were dissolved in 1 mL ethanol and stirred at 80˚C for 25 hours. After cooling to room temperature, the solution was concentrated under reduced pressure to produce a red-orange residue. The crude product was partially dissolved in acetonitrile, and filtered through syringe filter, followed by purification by reverse phase CombiFlash (C-18 column) with a 20-minute gradient of water/methanol. The fractions were combined and lyophilized to produce an off-white solid, **5** (32.3 mg, 14% yield). The pure product was characterized by ^{1}H-NMR and ^{13}C-NMR in $CDCl_3$ and $(CD_3)_2SO$ as well as HRMS. An interesting observation: in $CDCl_3$, the iminium of **5** is observed and in $(CD_3)_2SO$, the enamine is observed.

(**Figure 4.4**) 1H NMR (500 MHz, Chloroform-d) δ 8.00 – 7.96 (m, 2H), 7.81 – 7.76 (m, 2H), 7.49 – 7.41 (m, 5H), 7.23 (tt, J = 7.4, 1.2 Hz, 1H), 3.86 (s, 2H). (**Figure 4.5**) 1H NMR (500 MHz, DMSO-d6) δ 11.81 (s, 1H), 7.85 – 7.78 (m, 5H), 7.48 (t, J = 7.9 Hz, 2H), 7.41 (t, J = 7.6 Hz, 2H), 7.30 (dt, J = 20.5, 7.1 Hz, 2H), 6.01 (s, 1H). (**Figure 4.6**) 13C NMR (126 MHz, Chloroform-d) δ 170.40, 154.80, 138.27, 131.02, 130.89, 129.09, 126.14, 125.48, 119.26, 77.16, 39.83. (**Figure 4.7**) HRMS-ESI $[M + H]^+$ calculated for $C_{15}H_{12}N_2O$ 237.1022, found 237.1027

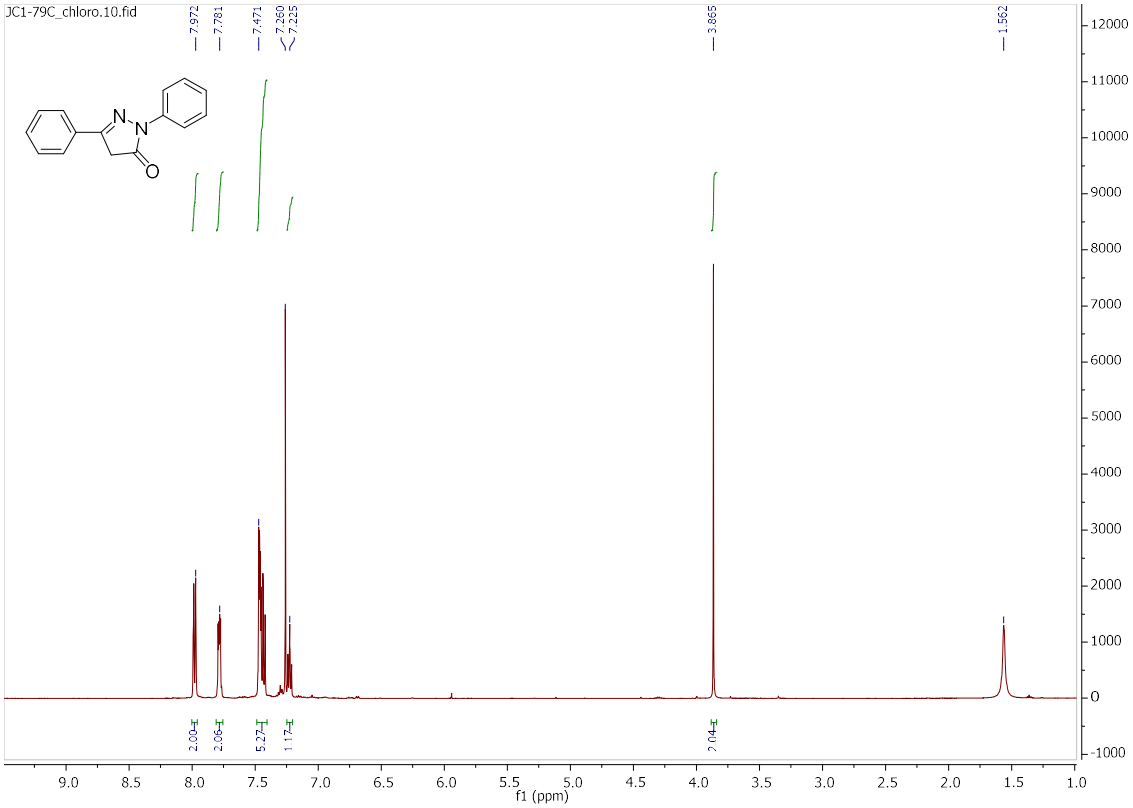

Figure 4.4: ^{1}H-NMR (500 MHz) in $CDCl_3$ of **5**.

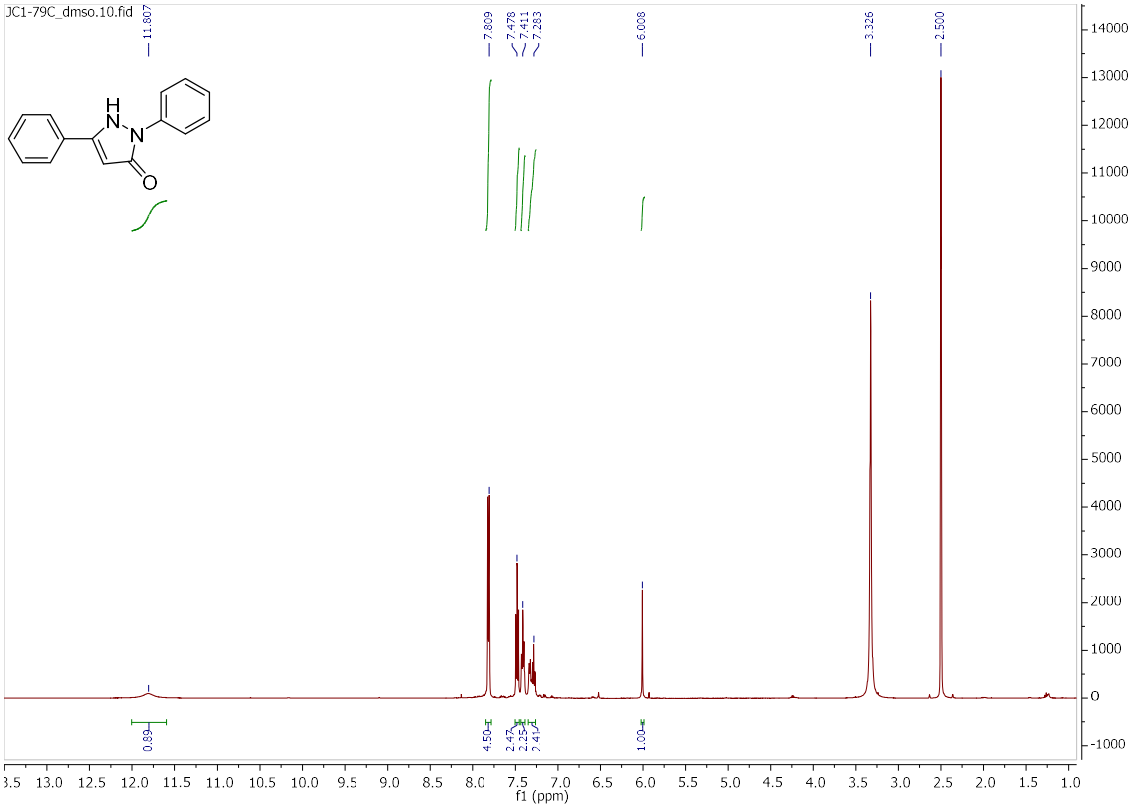

Figure 4.5: ^{1}H-NMR (500 MHz) in $(CD_3)_2SO$ of **5**.

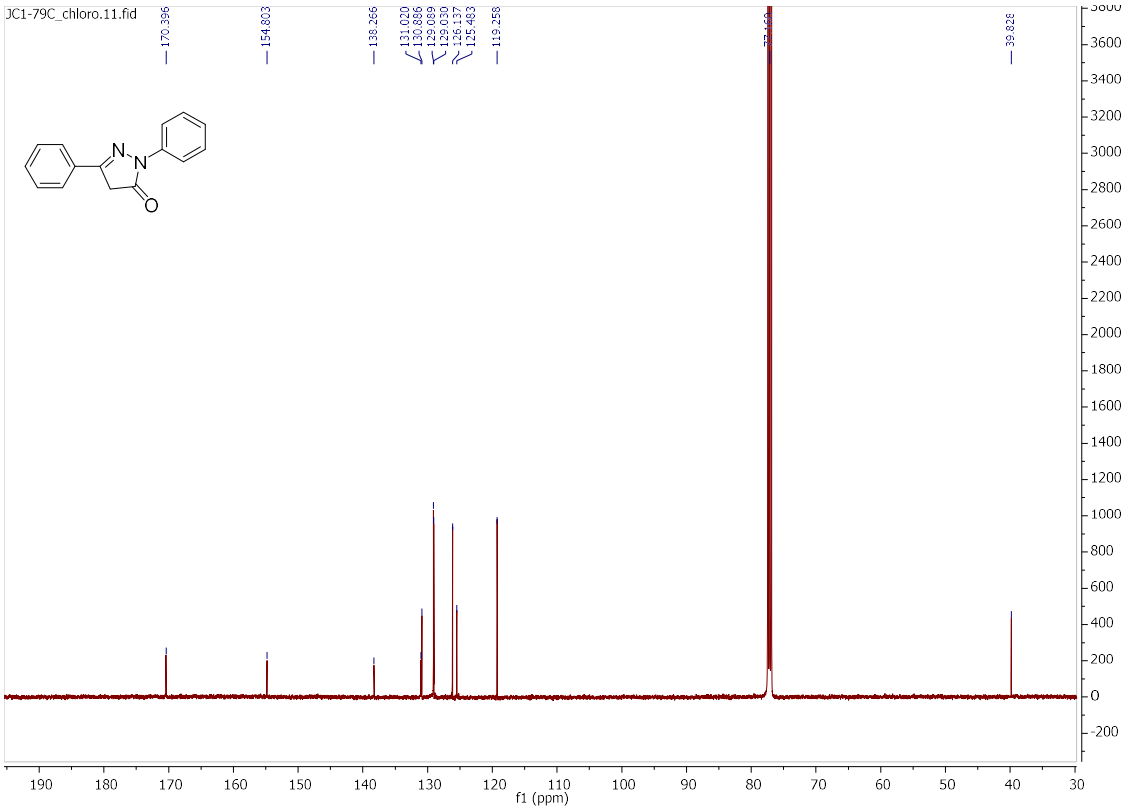

Figure 4.6: ^{13}C-NMR (500 MHz) in $CDCl_3$ of **5**.

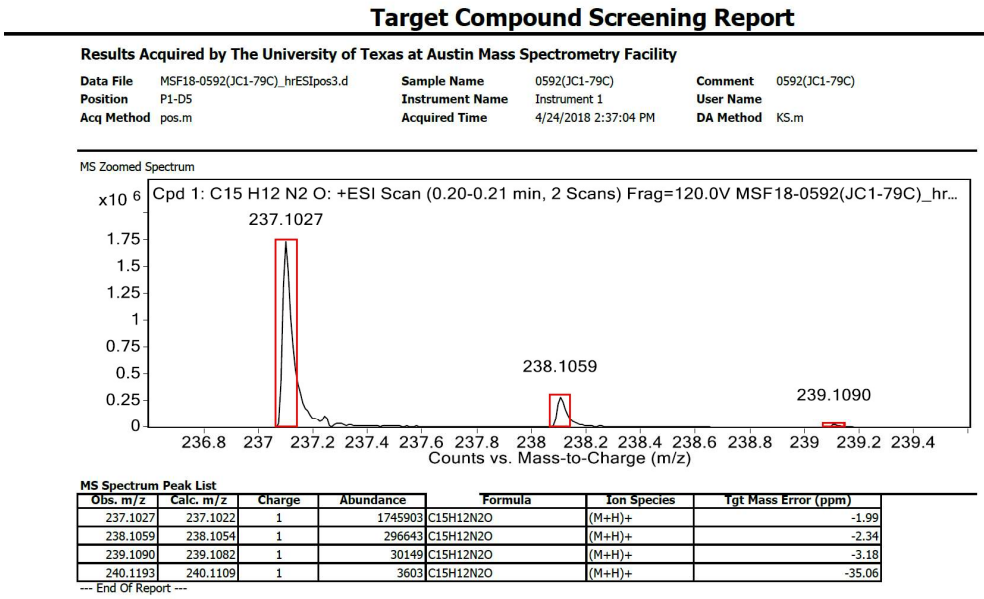

Figure 4.7: High Resolution Mass Spectrum (ESI positive mode) of **5.**

4.2.5 Scheme 6 Test Reaction

Phenyl hydrazine (0.498 mmol, 1.1 eq.) was dissolved in 1.00 mL ethanol, followed by addition of ethyl acetoacetate (0.435 mmol, 1.0 eq.) and sodium acetate (0.546 mmol, 1.3 eq.). The solution was heated while stirring at 75˚C overnight, and the solution turned a burnt orange color. Characterization by TLC showed two new product formations. The solution was extracted with DCM and concentrated under reduced pressure to produce an orange solid. The solution was purified by column chromatography (packed in hexanes, run in 1:1 to 1:4 hexane:ethyl acetate). The two products were collected, concentrated under reduced pressure, and characterized by ^{1}H-NMR. The desired product, **6**, was determined to be the first product to elude from the column, and was further characterized by ^{1}H-NMR, ^{13}C-NMR, and HRMS (0.101 g, 43.6% yield)

(**Figure 4.8**) 1H NMR (500 MHz, Chloroform-d) δ 7.85 (d, J = 8.1 Hz, 2H), 7.38 (t, J = 8.0 Hz, 2H), 7.17 (t, J = 7.4 Hz, 1H), 3.41 (s, 2H), 2.18 (s, 3H), 1.25 (s, 1H). (**Figure 4.9**) 13C NMR (126 MHz, Chloroform-d) δ 170.69, 156.43, 138.13, 128.92, 125.15, 118.98, 43.20, 29.80, 17.11. (**Figure 4.10**) HRMS-ESI $[M + H]^+$ calculated for $C_{10}H_{10}N_2O$ 175.0866, found 175.0869. (**Figure 4.11**) HRMS-ESI $[M - H]^-$ calculated for $C_{10}H_{10}N_2O$ 173.0730, found 173.0717.

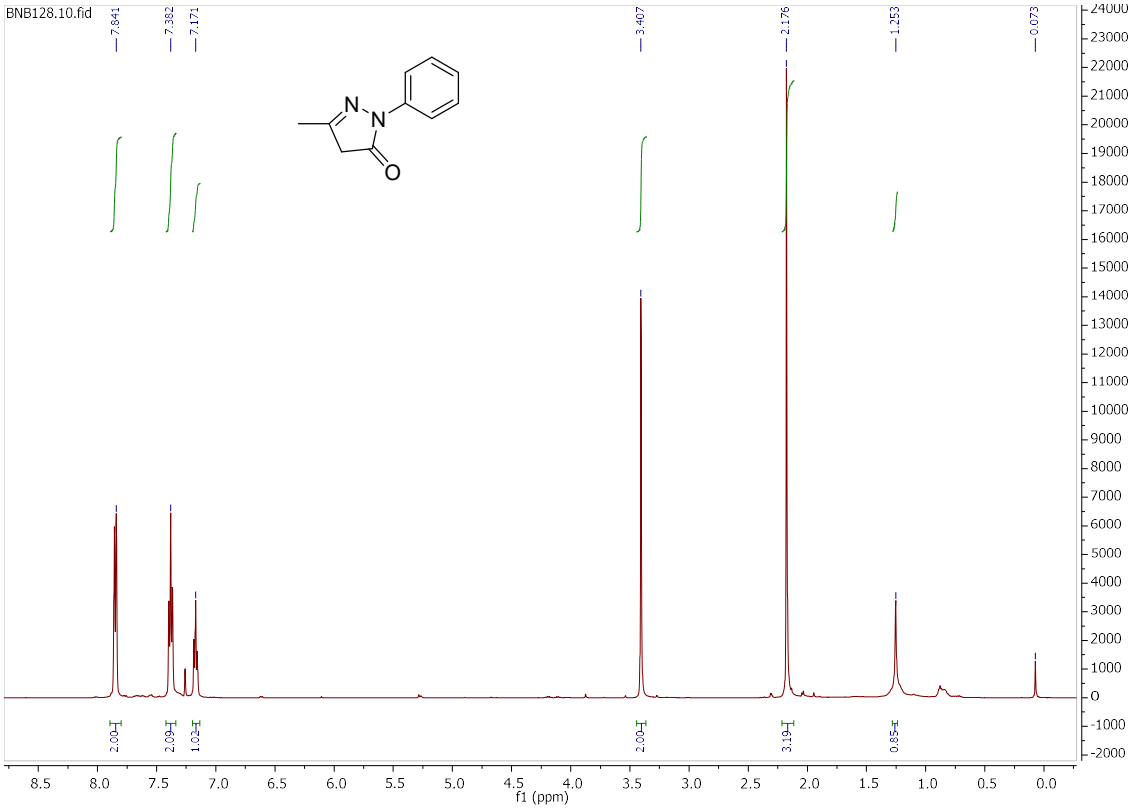

Figure 4.8: ^{1}H-NMR (500 MHz) in $CDCl_3$ of **6**.

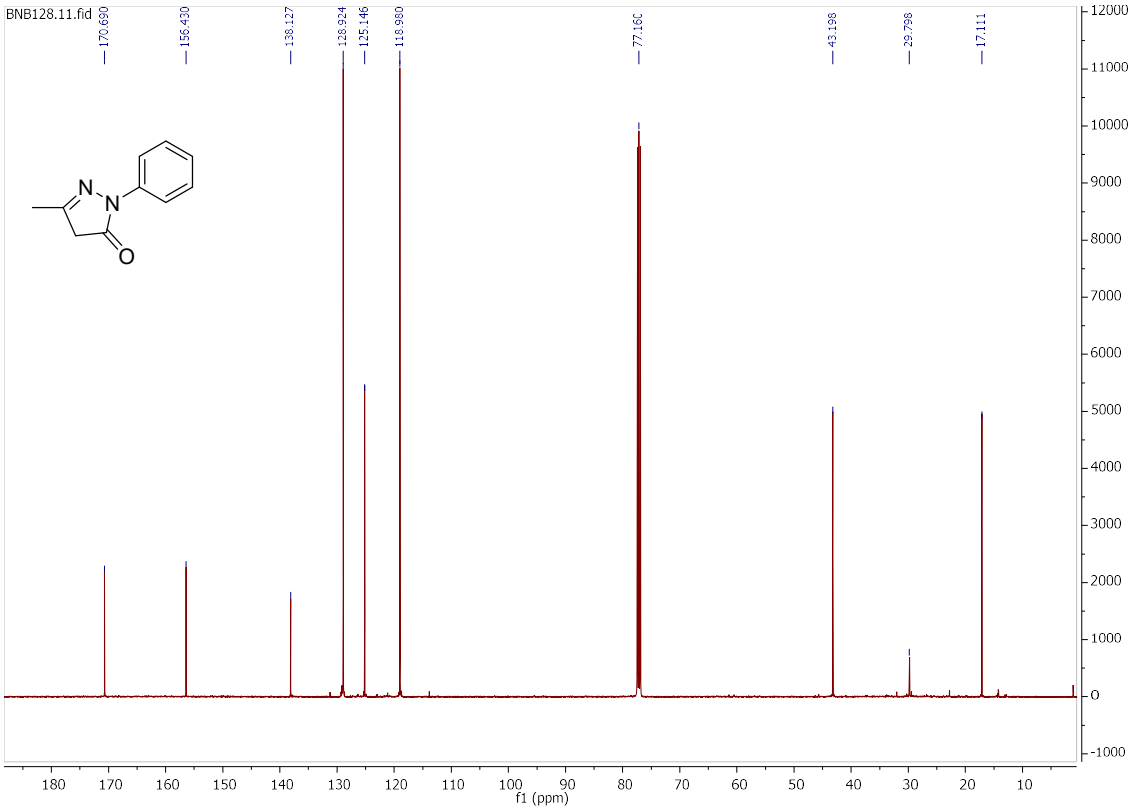

Figure 4.9: ^{13}C-NMR (500 MHz) in $CDCl_3$ of **6**.

Target Compound Screening Report

Results Acquired by The University of Texas at Austin Mass Spectrometry Facility

Data File	MSF18-0588(BNB128)_hrESIpos2.d	**Sample Name**	0588(BNB128)	**Comment**	0588(BNB128)
Position	P1-A6	**Instrument Name**	Instrument 1	**User Name**	
Acq Method	pos.m	**Acquired Time**	4/23/2018 9:54:27 AM	**DA Method**	KS.m

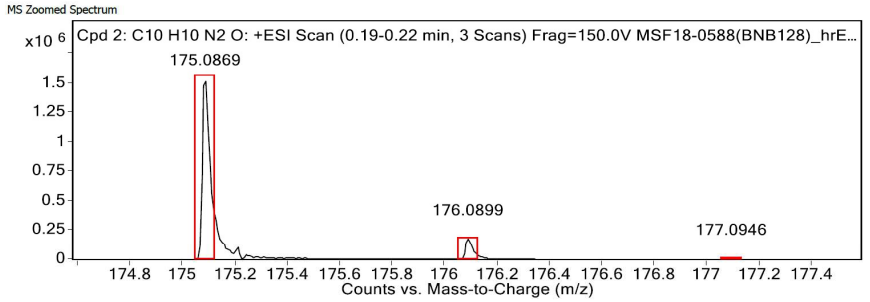

MS Spectrum Peak List

Obs. m/z	Calc. m/z	Charge	Abundance	Formula	Ion Species	Tgt Mass Error (ppm)
175.0869	175.0866	1	1555226	C10H10N2O	(M+H)+	-1.97
176.0899	176.0896	1	181750	C10H10N2O	(M+H)+	-1.6
177.0946	177.0921	1	14359	C10H10N2O	(M+H)+	-13.96
178.0996	178.0946	1	1138	C10H10N2O	(M+H)+	-28.34

--- End Of Report ---

Figure 4.10: High Resolution Mass Spectrum (ESI positive mode) of **6**.

Target Compound Screening Report

Results Acquired by The University of Texas at Austin Mass Spectrometry Facility

Data File	MSF18-0588(BNB128)_hrESIneg1.d	**Sample Name**	0588(BNB128)	**Comment**	0588(BNB128)
Position	P1-A6	**Instrument Name**	Instrument 1	**User Name**	
Acq Method	neg.m	**Acquired Time**	4/23/2018 9:42:24 AM	**DA Method**	KS.m

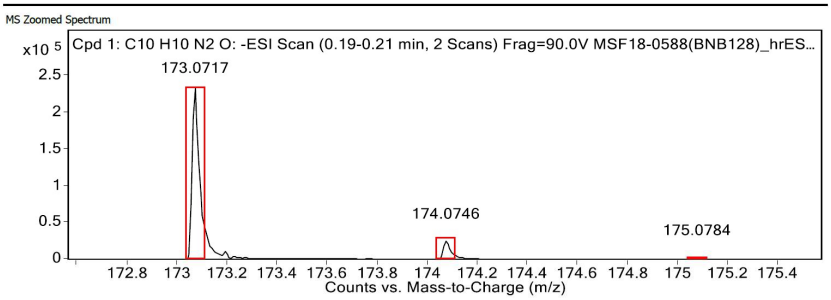

MS Spectrum Peak List

Obs. m/z	Calc. m/z	Charge	Abundance	Formula	Ion Species	Tgt Mass Error (ppm)
173.0717	173.0720	1	234118	C10H10N2O	(M-H)-	1.95
174.0746	174.0750	1	24616	C10H10N2O	(M-H)-	2.31
175.0784	175.0776	1	2162	C10H10N2O	(M-H)-	-4.86
176.0074	176.0800	1	129	C10H10N2O	(M-H)-	412.48

--- End Of Report ---

Figure 4.11: High Resolution Mass Spectrum (ESI negative mode) of **6**.

4.2.6 Scheme 9 Test Reaction

2-Amino benzaldehyde (0.419 mmol, 1.0 eq.) was dissolved in 1.0 mL methanol, followed by the addition of methyl α-bromophenylacetate (0.413 mmol, 1.0 eq.), and potassium phosphate tribasic (0.416 mmol, 1.0 eq.). Solution heated at 62˚C overnight, and characterized by TLC (3:1 hexane:ethyl acetate) to show a small amount of starting material and the development of one main product. The solution was diluted in ethyl acetate, washed with brine, a few drops of 3M HCl added, and concentrated under reduced pressure. Solution characterized by LC/MS to show amine displacement of the bromine, and no **9** formed.

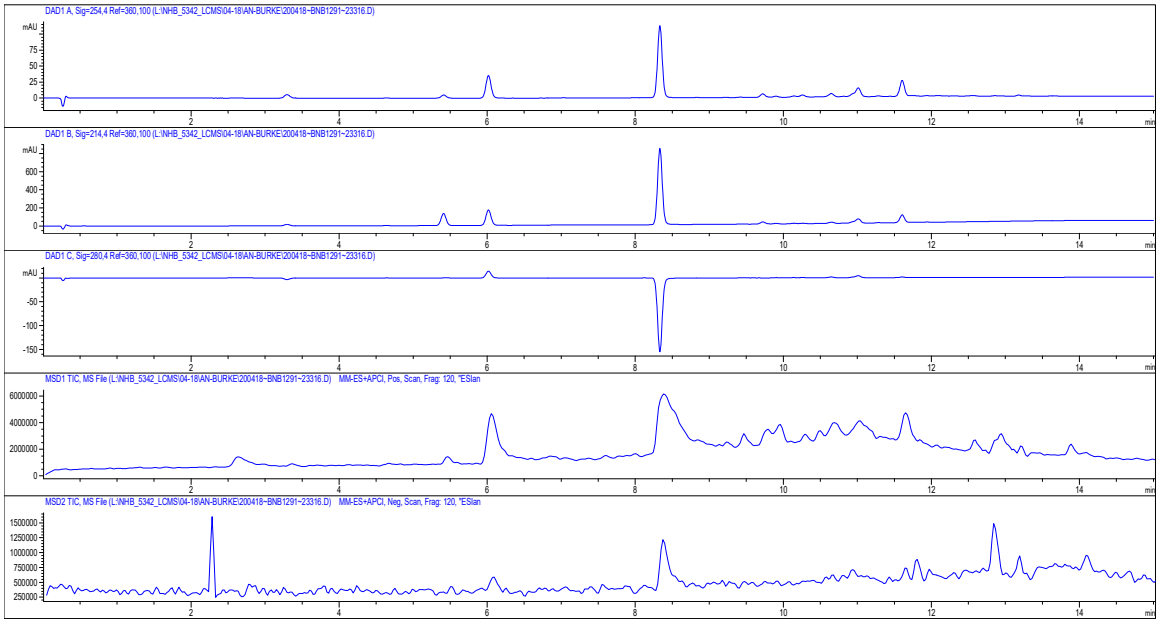

Figure 4.12: LC/MS data of Scheme 9. LC traces: at 254 nm, 214 nm, and 280 nm (frames 1-3). Mass detection: ESI/APCI positive ionization (frame 4), ESI/APCI negative ionization (frame 5).

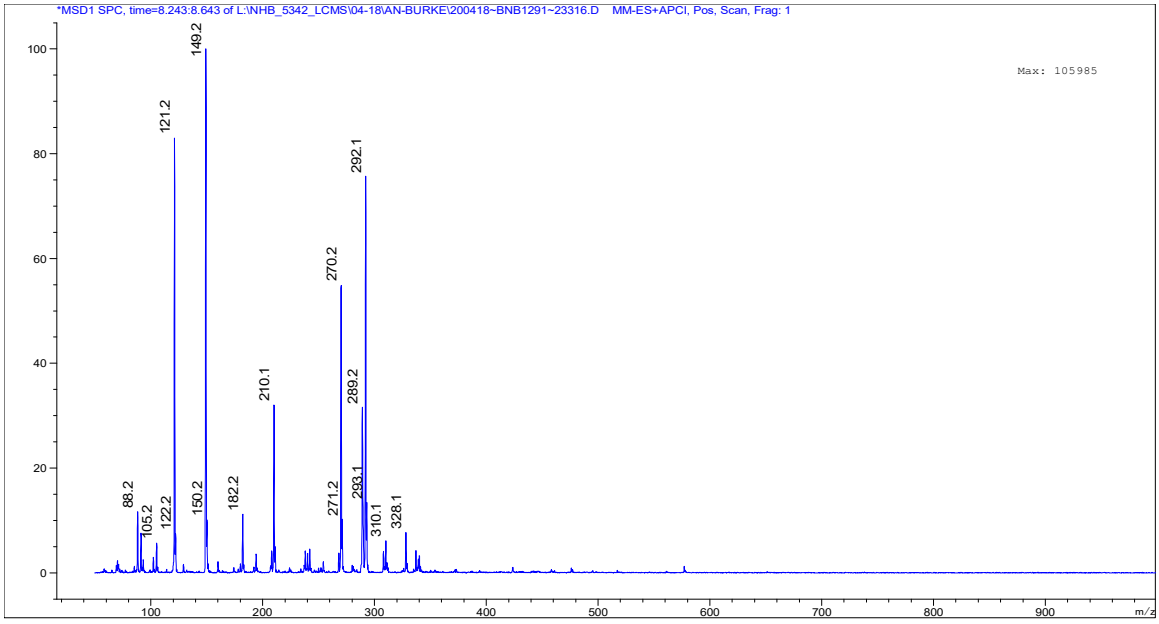

Figure 4.13: ESI/APCI positive ionization mass spectrum from 8.2 to 8.6 min.

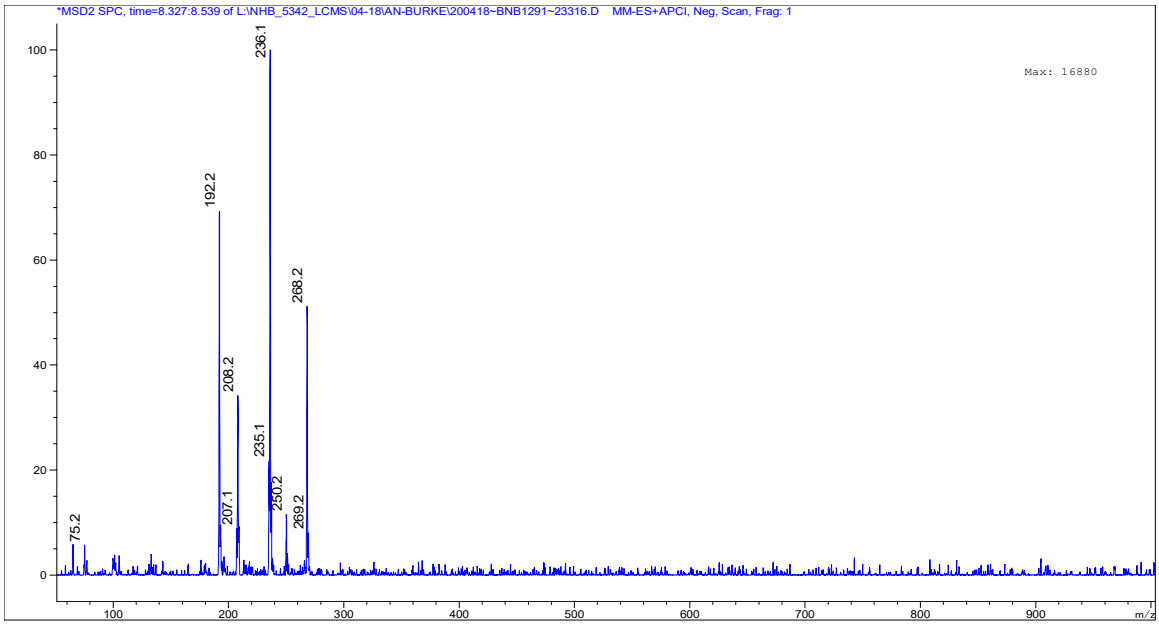

Figure 4.14: ESI/APCI negative ionization mass spectrum from 8.3 to 8.6 min.

4.3 MONOMER SYNTHESIS

4.3.1 Plan 1

4.3.1.1 Claisen Reaction (10)

Following a protocol laid out by Rostovskii, et al., diisopropylamine (24.3 mmol, 2.2 eq.) was added to a flame-dried RBF of 12 mL dry THF on dry ice/acetone bath under argon. n-Butyllithium (23.8 mmol, 2.1 eq.) was added dropwise to the diisopropylamine solution and was rapidly stirred for 15 minutes.[8] Dry ethyl acetate (dried over sieves for several days) (24.6 mmol, 2.2 eq.) added quickly to the solution, and stirred an additional 15 minutes. In a second flame-dried RBF, methyl 4-nitrobenzoate (11.1 mmol, 1.0 eq.) was dissolved in 7 mL THF, then added dropwise to the first solution, and the reaction was monitored by TLC (2:1 hexane:ethyl acetate). After 30 minutes, the solution was quenched with 12 mL 20% HCl, then allowed to warm to room temperature. The solution was extracted with ether, washed with sat. $NaHCO_3$, H_2O, brine, dried with Na_2SO_4, and concentrated under reduced pressure to produce a thick orange oil. Compound dry loaded onto column packed in hexanes, and eluted with 6:1 hexane:ethyl acetate. Pure product was collected and concentrated under reduced pressure to produce a yellow solid, **10**, which was characterized by ^{1}H-NMR, ^{13}C-NMR, and HRMS. (0.922 g, 35.2% yield)

(**Figure 4.15**) 1H NMR (500 MHz, Chloroform-d) δ 12.55 (s, 1H), 8.35 – 8.29 (m, 1H), 8.29 – 8.22 (m, 2H), 8.13 – 8.08 (m, 1H), 7.95 – 7.89 (m, 2H), 5.75 (s, 1H), 4.29 (q, J = 7.2 Hz, 2H), 4.21 (q, J = 7.2 Hz, 1H), 4.03 (s, 1H), 1.34 (t, J = 7.1 Hz, 3H), 1.25 (t, J = 7.2 Hz, 1H). (**Figure 4.16**) 13C NMR (126 MHz, Chloroform-d) δ 191.21, 172.75, 168.39, 166.81, 150.74, 149.35, 140.46, 139.45, 129.71, 127.08, 124.11, 123.87, 90.36, 61.98, 60.99, 46.34, 14.34, 14.16. (**Figure 4.17**) HRMS-ESI $[M + Na]^+$ calculated for $C_{11}H_{11}NO_5$ 260.0529, found 260.0523.

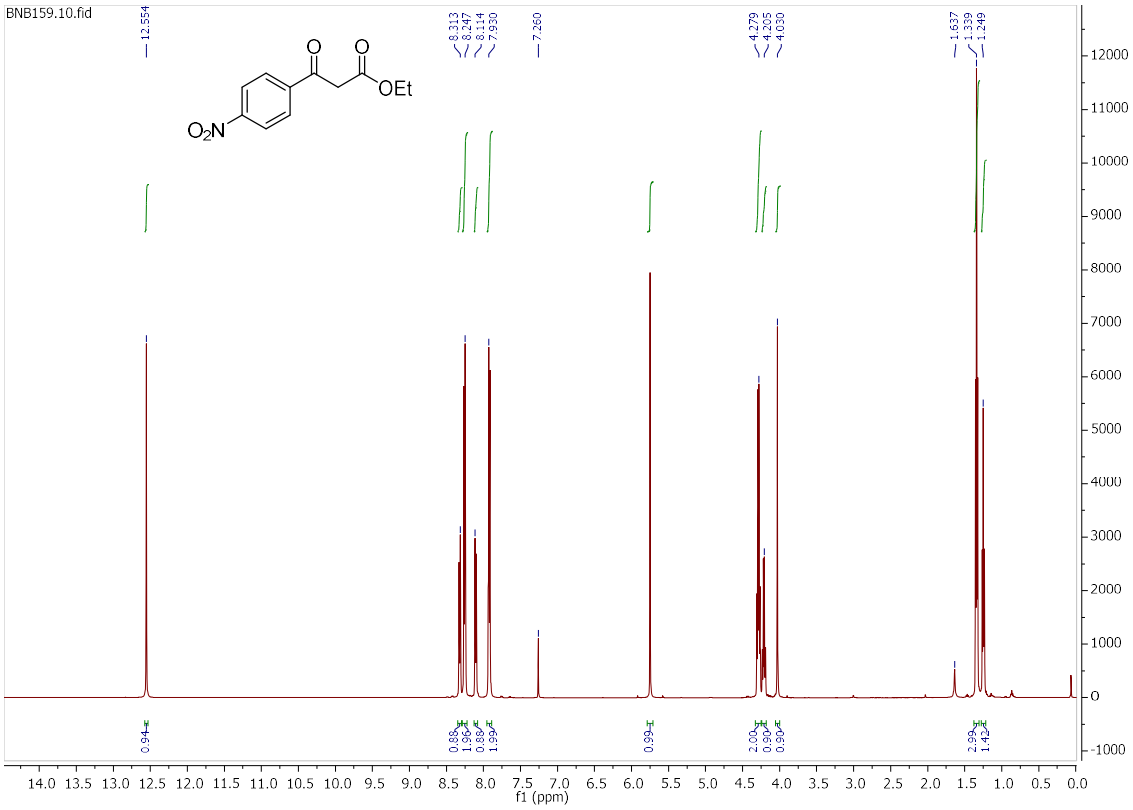

Figure 4.15: ^{1}H-NMR (500 MHz) in $CDCl_3$ of **10**.

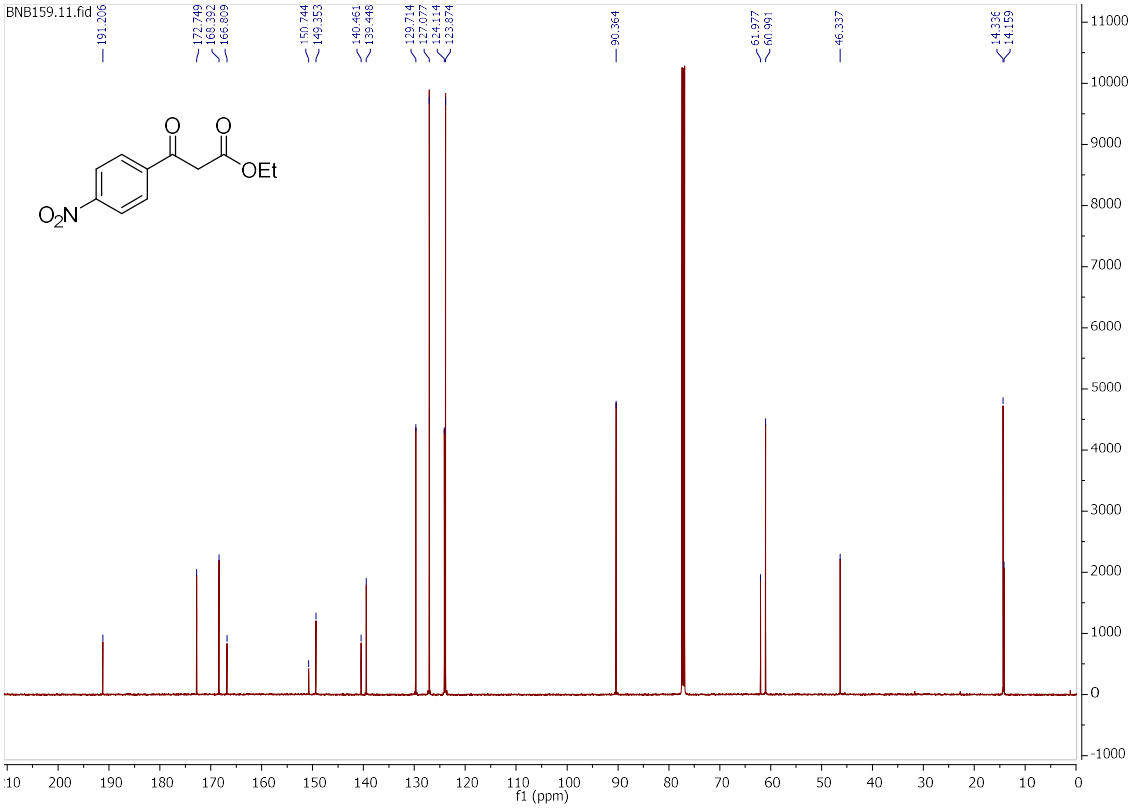

Figure 4.16: ^{13}C-NMR (500 MHz) in $CDCl_3$ of **10**.

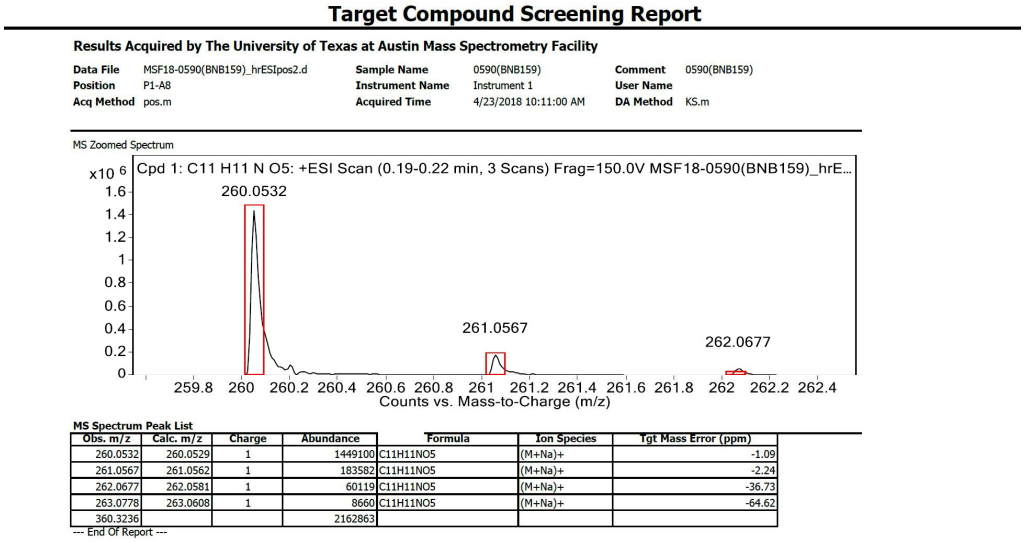

Figure 4.17: High Resolution Mass Spectrum (ESI positive mode) of **10**.

4.3.1.2 Nitro Reduction (11)

Claisen product (0.124 mmol) was dissolved in 1 mL dichloroethane. 10% platinum on activated carbon (20% by weight) added to solution, and H_2(g) was bubbled through the solution three times before allowing to stir under H_2(g). The reaction was monitored closely by LC/MS for the consumption of **10** and the production of **11**, as well as the undesired alcohol product. After 30 minutes, the solution was filtered through syringe filter and concentrated under reduced pressure to produce a yellow oil. Product was then dissolved in 1:1 water:acetonitrile and purified by HPLC. Relevant fractions were collected, concentrated under reduced pressure, and lyophilized to produce a yellow solid, **11**, which was characterized by ^{1}H-NMR, ^{13}C-NMR, and HRMS. (20.4% yield)

(**Figure 4.18**) 1H NMR (500 MHz, Chloroform-d) δ 7.82 – 7.74 (m, 2H), 6.67 – 6.61 (m, 2H), 4.20 (q, J = 7.1 Hz, 2H), 3.89 (s, 2H), 1.25 (t, J = 7.0 Hz, 4H). (**Figure 4.19**)

13C NMR (126 MHz, Chloroform-d) δ 190.63, 168.25, 151.77, 131.30, 126.71, 113.98, 61.47, 45.76, 14.25, 1.16. (**Figure 4.20**) HRMS-ESI $[M + H]^+$ calculated for $C_{11}H_{13}NO_3$ 208.0968, found 208.0970.

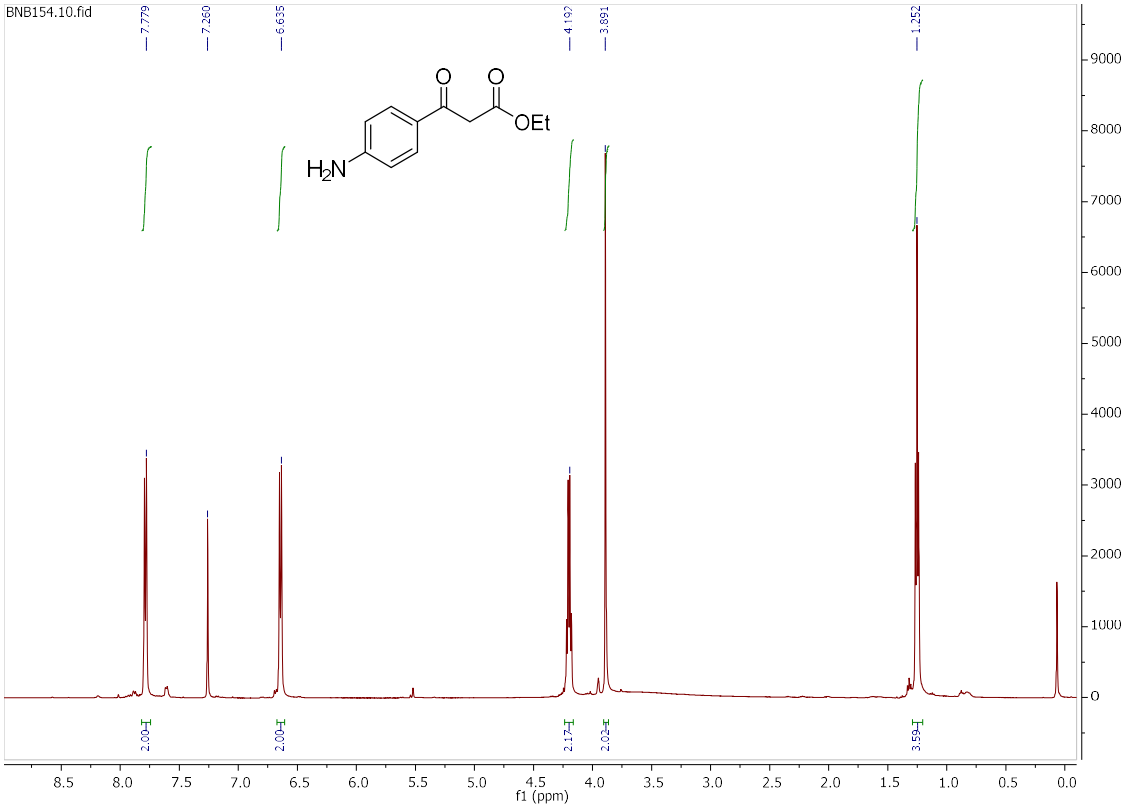

Figure 4.18: ^{1}H-NMR (500 MHz) in $CDCl_3$ of **11**.

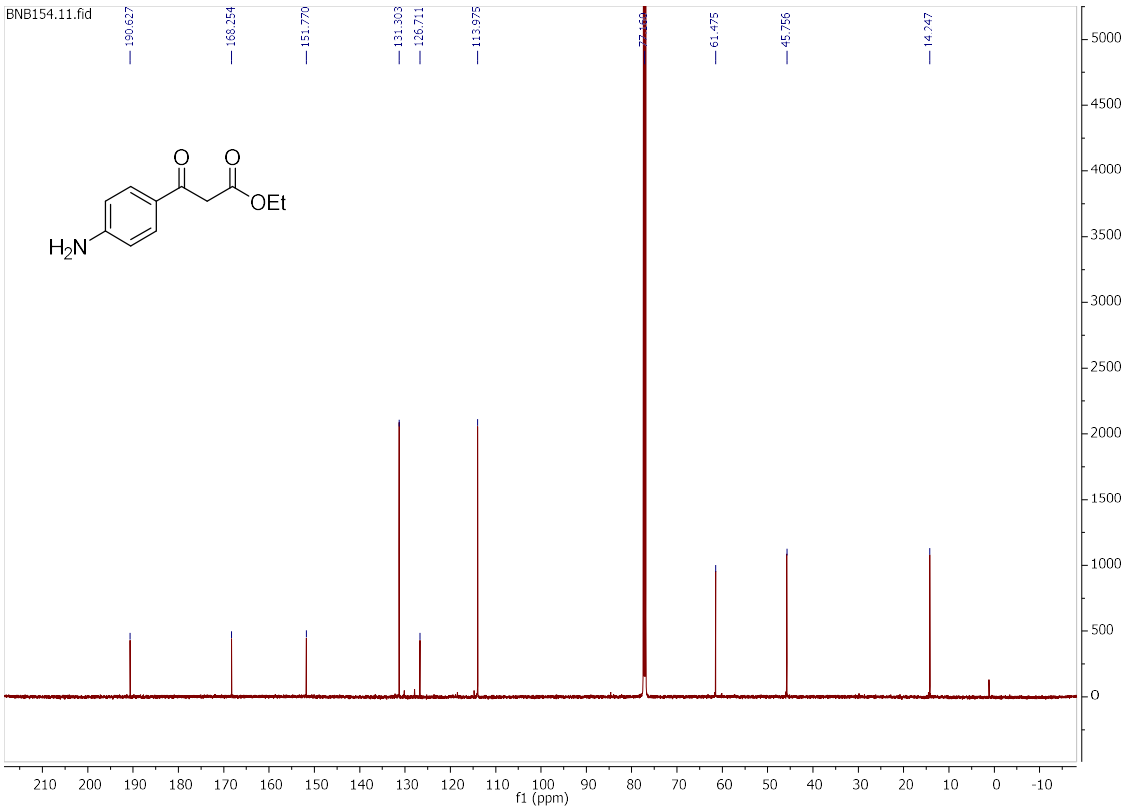

Figure 4.19: ^{13}C-NMR (500 MHz) $CDCl_3$ of **11**.

Target Compound Screening Report

Results Acquired by The University of Texas at Austin Mass Spectrometry Facility

Data File	MSF18-0589(BNB154)_hrESIpos4.d	**Sample Name**	0589(BNB154)	**Comment**	0589(BNB154)
Position	P1-A7	**Instrument Name**	Instrument 1	**User Name**	
Acq Method	pos.m	**Acquired Time**	4/23/2018 10:04:56 AM	**DA Method**	KS.m

MS Zoomed Spectrum

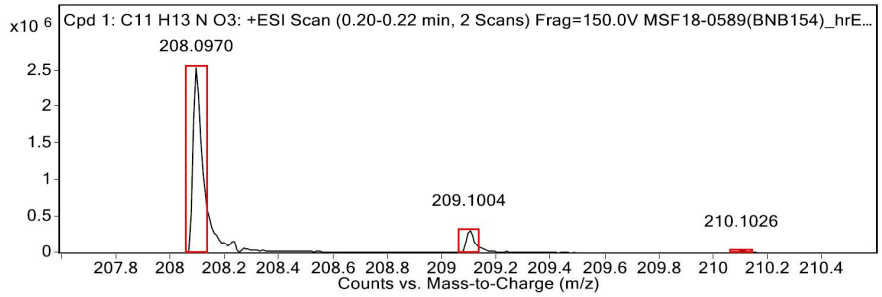

MS Spectrum Peak List

Obs. m/z	Calc. m/z	Charge	Abundance	Formula	Ion Species	Tgt Mass Error (ppm)
208.0970	208.0968	1	2554519	C11H13NO3	(M+H)+	-1
209.1004	209.1000	1	322012	C11H13NO3	(M+H)+	-1.83
210.1026	210.1022	1	35681	C11H13NO3	(M+H)+	-1.78
211.1050	211.1048	1	2304	C11H13NO3	(M+H)+	-1.14

--- End Of Report ---

Figure 4.20: High Resolution Mass Spectrum (ESI positive mode) of **11**.

4.3.1.3 Diazotization (M6)

Following protocol provided by Kuznetsova, et al., **11** (0.053 mmol, 1.0 eq.) was dissolved in 0.5 mL conc. HCl and cooled to 0˚C.[9] In a separate flask, sodium nitrate (0.085 mmol, 1.6 eq.) dissolved in 0.1 mL water, then added dropwise to the first solution, and stirred at 0˚C for 30 minutes, then cooled back to -5˚C. A solution of $SnCl_2 \cdot H_2O$ in 0.15 mL conc. HCl cooled to -18˚C (on dry ice/glycol bath) was slowly added to the first solution. After addition, the solution was allowed to gently warm to 5˚C and stirred overnight. No crystals formed, as outlined in the provided protocol, and after characterization by LC/MS, only undesired products were observed.

4.3.1.4 Test Diazotization (12 & 13)

11 (0.267 mmol, 1.0 eq.) was dissolved in 0.80 mL 1M HCl, and cooled to -5˚C. In a separate flask, sodium nitrate (0.268 mmol, 1.0 eq.) dissolved in 106.0 µL to form a 2.5M solution, which was added dropwise to the first solution. Solution allowed to stir for 5 minutes at -5˚C, then characterized by LC/MS, and base was added to the solution to neutralize any sodium nitrate left in solution. Salicylic acid (0.309 mmol, 1.2 eq) was dissolved in 400 µL 2M NaOH, then the first solution added dropwise to the salicylic acid solution, maintaining basic pH by litmus paper. Solution acidified with 1M HCl, and precipitate filtered off, and characterized by LC/MS to show the diazotization moiety attacked the enol position of another **11**.

4.3.2 Plan 2

4.3.2.1 Fischer Esterification (14)

4-Hydrazinobenzoic acid (6.586 mmol) was put into a RBF, and 15 mL 5% H_2SO_4/dry EtOH (ethanol dried over sieves for several days) added to create a suspension, which was stirred rapidly while brought to a reflux over 16 hours. As the product is soluble, the suspension produced a yellow solution as the reaction occurred. After cooling to room temperature, the solution was extracted with ethyl acetate, washed twice each with brine and sat. $NaHCO_3$, dried over Na_2SO_4, and concentrated under reduced pressure to produce a yellow solid, **14**, which was characterized by ^{1}H-NMR and LC/MS. (0.569 g, 48.0% yield)

(**Figure 4.21**) 1H NMR (400 MHz, Methanol-d4) δ 7.84 – 7.78 (m, 2H), 6.83 – 6.78 (m, 2H), 4.28 (q, J = 7.1 Hz, 2H), 1.35 (t, J = 7.1 Hz, 3H).

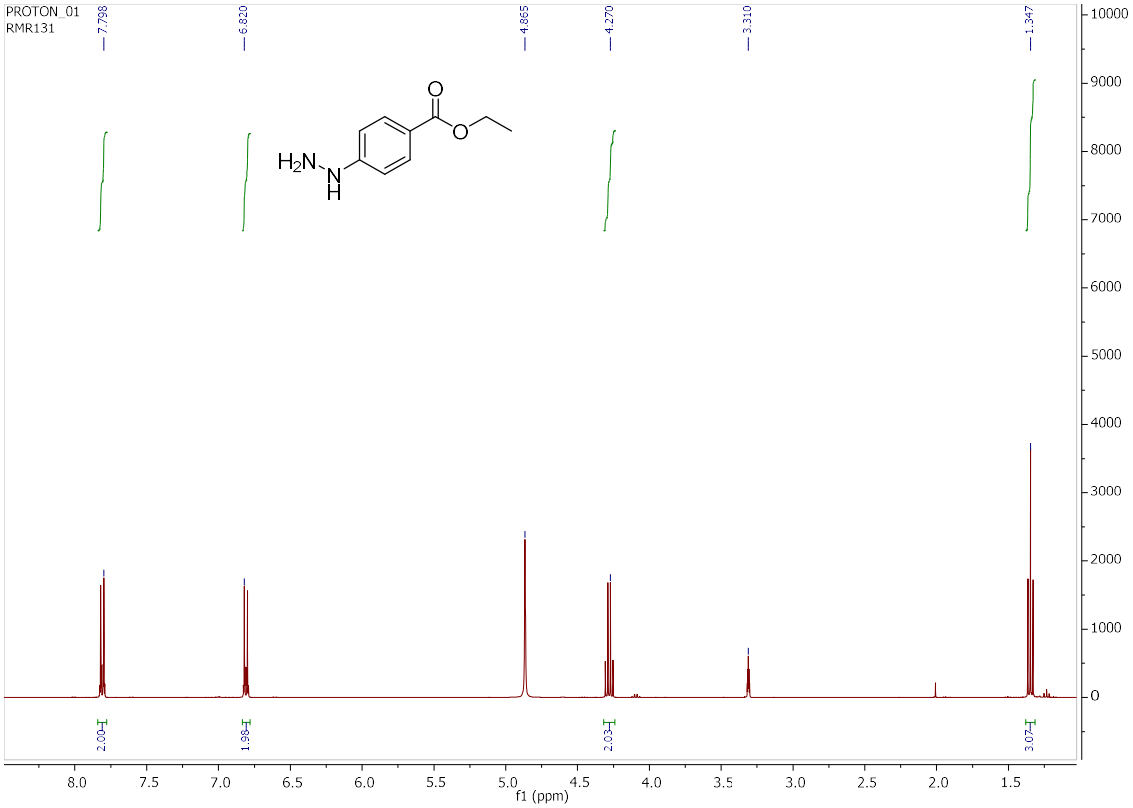

Figure 4.21: ^{1}H-NMR (400 MHz) in CD_3OD of **14**.

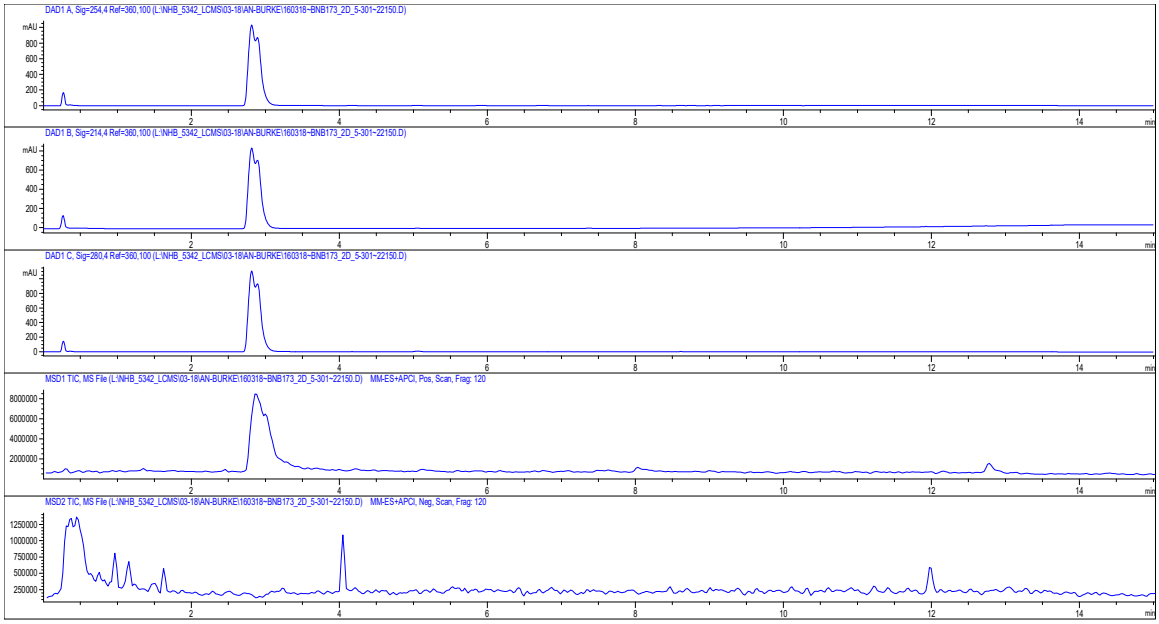

Figure 4.22: LC/MS of **14**. LC traces: at 254 nm, 214 nm, and 280 nm (frames 1-3). Mass detection: ESI/APCI positive ionization (frame 4), ESI/APCI negative ionization (frame 5).

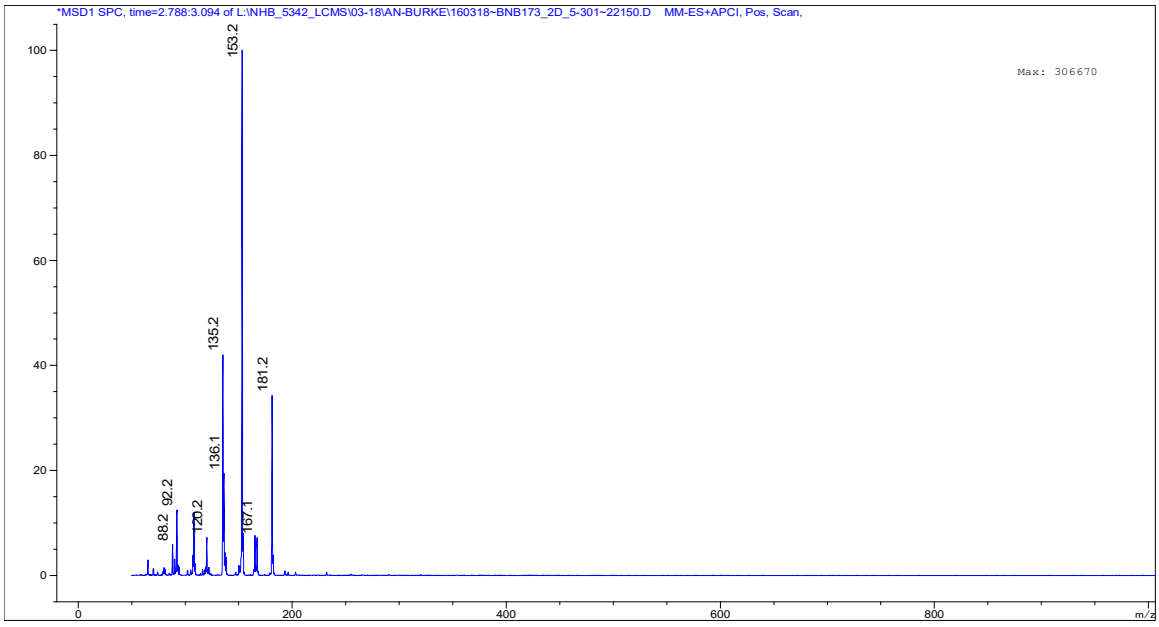

Figure 4.23: ESI/APCI positive ionization mass spectrum from 2.8 to 3.1 min of **14**.

4.3.2.2 Tri-Boc Protection (15)

Following protocol set by Loog, et al., **14** (2.656 mmol, eq.) was partially dissolved in 5 mL dry acetonitrile (dried over Na_2SO_4 for several days) under argon.[17] In a separate flask, di-tert-butyl dicarbonate (9.704 mmol, 3.7 eq.) was dissolved in 2.5 mL dry acetonitrile, then added to the first solution to stir at room temperature for at least one hour. Dimethylaminopyridine (0.105 mmol, 0.04 eq.) was dissolved in a third flask in 0.15 mL acetonitrile and added to the first solution, then heated at 60˚C for 24 hours. Reaction was monitored by TLC (2:1 ethyl acetate:hexanes) and LC/MS, by which **14,** mono-Boc, di-Boc, and **15** were observed. After the disappearance of **14**, the reaction was cooled to room temperature, the solution was extracted with ether, washed with 1:1 1M $KHSO_4$:brine, sat. $NaHCO_3$, brine, dried with Na_2SO_4, and concentrated under reduced pressure. Desired **15** and di-Boc side product could be isolated using a slow gradient of water:acetonitrile by CombiFlash. Fractions were combined, organics were evaporated under reduced pressure, extracted from the aqueous layer with ether, followed by a final concentration under reduced pressure. Di-Boc product produced a yellow solid, and **15** produced an orange viscous gel (0.661 g, 51.9% yield).

(**Figure 4.23**)1H NMR (500 MHz, Chloroform-d) δ 7.99 (d, J = 8.8 Hz, 2H), 7.47 (s, 2H), 4.35 (q, J = 7.1 Hz, 2H), 1.46 (s, 27H), 1.38 (t, J = 7.2 Hz, 3H). (**Figure 4.24**) 13C NMR (126 MHz, Chloroform-d) δ 166.22, 151.60, 150.10, 144.91, 130.22, 84.21, 61.04, 28.21, 28.01, 14.46. (**Figure 4.25**) HRMS-ESI $[M + Na]^+$ calculated for $C_{24}H_{36}N_2O_8$ 503.2364, found 503.2364.

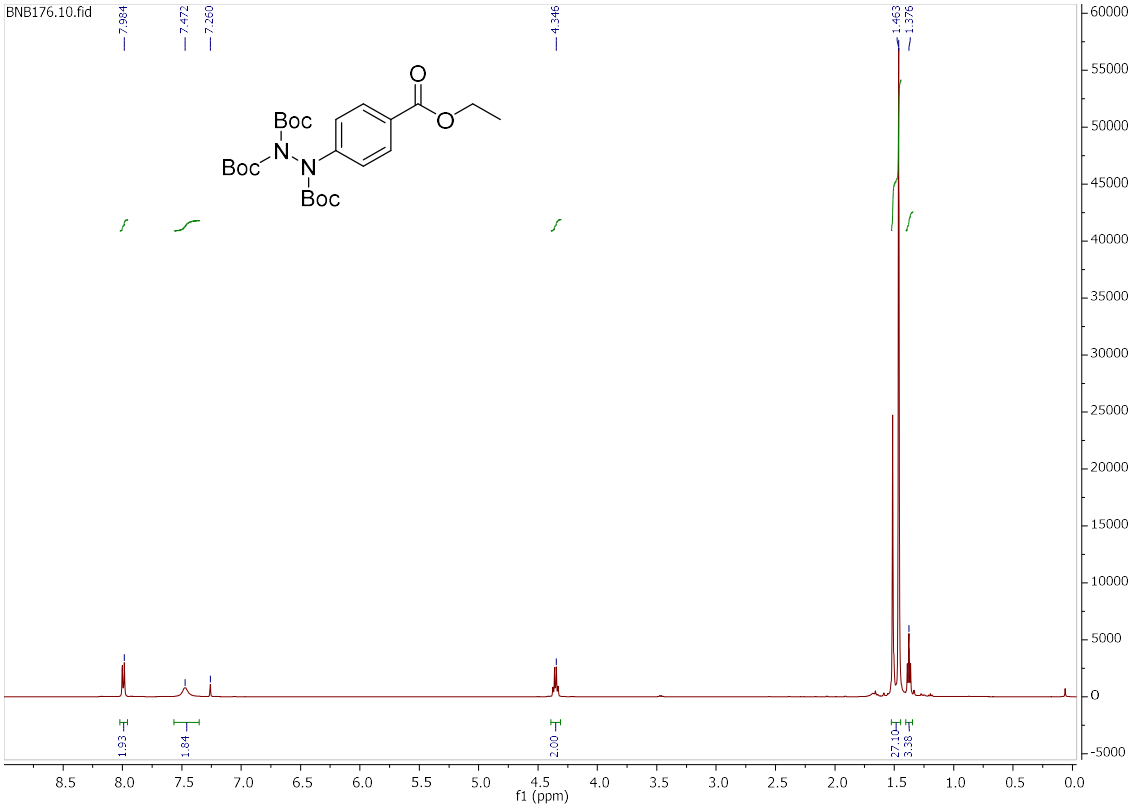

Figure 4.24: ^{1}H-NMR (500 MHz) in $CDCl_3$ of **15**.

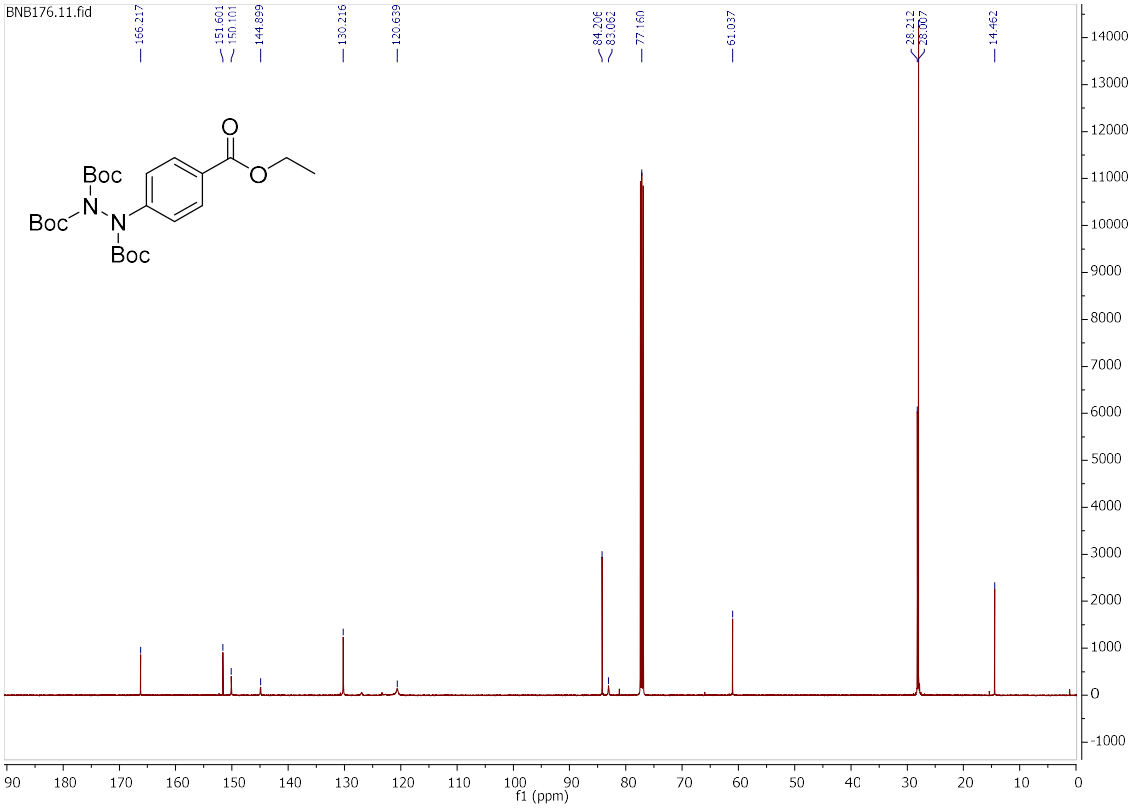

Figure 4.25: ^{13}C-NMR (500 MHz) in $CDCl_3$ of **15**.

Target Compound Screening Report

Results Acquired by The University of Texas at Austin Mass Spectrometry Facility

Data File	MSF18-0591(BNB176)_hrESIpos2.d	**Sample Name**	0591(BNB176)	**Comment**	0591(BNB176)
Position	P1-A9	**Instrument Name**	Instrument 1	**User Name**	
Acq Method	pos.m	**Acquired Time**	4/23/2018 10:13:59 AM	**DA Method**	KS.m

MS Zoomed Spectrum

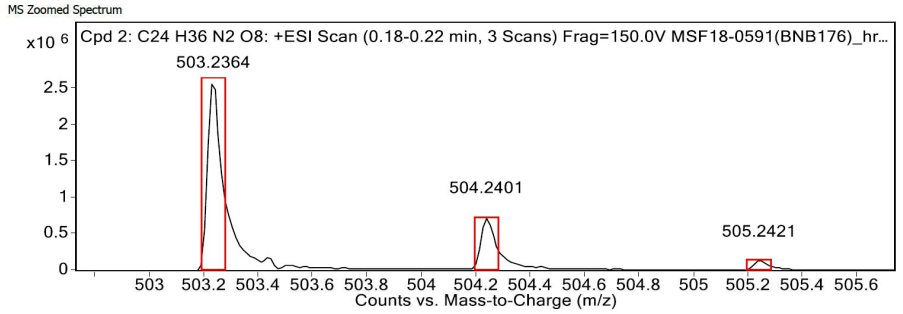

MS Spectrum Peak List

Obs. m/z	Calc. m/z	Charge	Abundance	Formula	Ion Species	Tgt Mass Error (ppm)
503.2364	503.2364	1	2648712	C24H36N2O8	(M+Na)+	0.06
504.2401	504.2396	1	730394	C24H36N2O8	(M+Na)+	-0.96
505.2421	505.2422	1	129985	C24H36N2O8	(M+Na)+	0.07
506.2455	506.2448	1	18029	C24H36N2O8	(M+Na)+	-1.4
507.2487	507.2473	1	4087	C24H36N2O8	(M+Na)+	-2.78
983.4839			17763554			

--- End Of Report ---

Figure 4.26: High Resolution Mass Spectrum (ESI positive mode) of **15**.

4.3.2.3 Claisen Reaction (18)

Diisopropylamine (4.545 mmol, 3.5 eq.) was added to a flame-dried RBF of 2.5 mL dry THF on a dry ice/acetone bath under argon. n-Butyllithium (4.750 mmol, 3.7 eq.) was added dropwise to the diisopropylamine solution and was rapidly stirred for 10 minutes. Dry ethyl acetate (dried over sieves for several days) (4.607 mmol, 3.5 eq.) added quickly to the solution, and stirred an additional 15 minutes. In a second flame-dried RBF, **15** (1.299 mmol, 1.0 eq.) was dissolved in 3.0 mL dry THF, then added dropwise to the first solution still at -79˚C. Solution stirred and gradually allowed to warm to room temperature by allowing the ice bath to melt. Reaction monitored by LC/MS, where **15**, tri-Boc Claisen (**16**), di-Boc starting material (**17**), and **18** were observed and monitored (**Figure 4.29-4.33**). After 5 hours, all of **15** was consumed, and the reaction was quenched

with 100 mL 100mM phosphate buffer. Precipitate formed upon quenching, and precipitate and solution were extracted with ether, washed with sat. $NaHCO_3$, H_2O, brine, dried with Na_2SO_4, and concentrated under reduced pressure to produce a yellow, impure solid. The solid was dissolved in acetonitrile and purified by CombiFlash. Fractions were combined, acetonitrile removed under reduced pressure, and the aqueous layer was extracted with diethyl ether, dried with Na_2SO_4, and finally concentrated under reduced pressure. Pure **18** was obtained as a yellow solid, which was characterized by ^{1}H-NMR, ^{13}C-NMR, and HRMS. (0.214 g, 40% yield)

(**Figure 4.26**) 1H NMR (500 MHz, Chloroform-d) δ 7.98 – 7.94 (m, 6H), 7.92 – 7.87 (m, 2H), 7.58 (d, J = 8.4 Hz, 2H), 7.45 – 7.40 (m, 6H), 6.76 (s, 2H), 4.34 (q, J = 7.1 Hz, 6H), 4.20 (q, J = 7.1 Hz, 2H), 3.95 (s, 2H), 1.58 – 1.41 (m, 52H), 1.37 (t, J = 7.1 Hz, 10H), 1.25 (t, J = 7.1 Hz, 4H). (**Figure 4.27**) 13C NMR (126 MHz, Chloroform-d) δ 166.41, 152.35, 142.76, 130.95, 129.31, 124.83, 117.45, 83.50, 81.29, 61.61, 60.87, 46.07, 28.40, 28.21, 14.49, 14.21. (**Figure 4.28**) HRMS-ESI $[M + H]^+$ calculated for $C_{12}H_{30}N_2O_7$ 423.2126, found 423.2132.

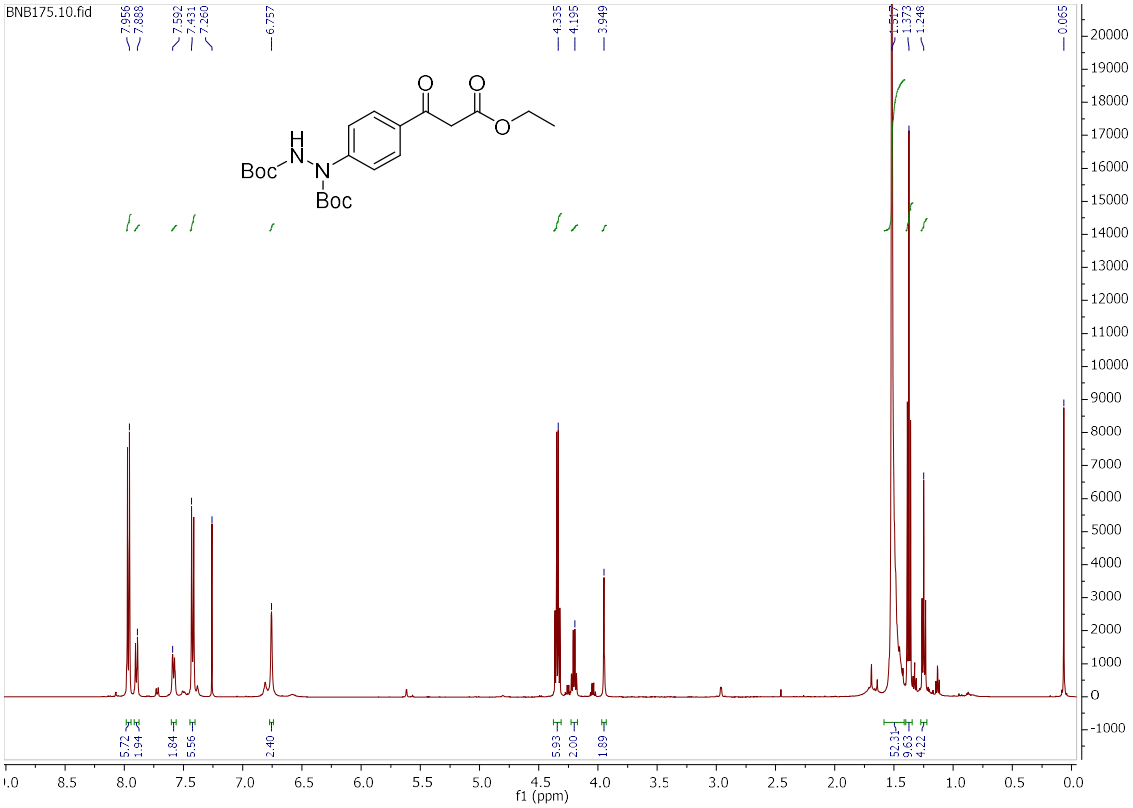

Figure 4.27: ^{1}H-NMR (500 MHz) in $CDCl_3$ of **18**.

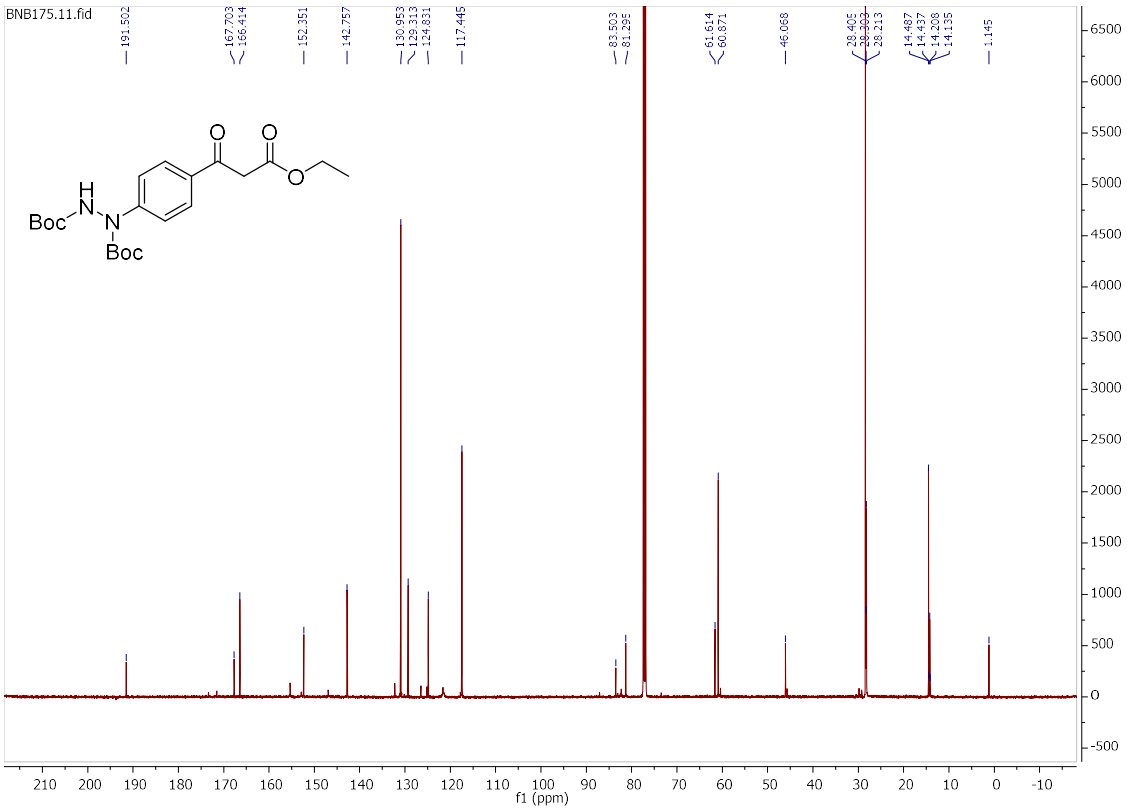

Figure 4.28: ^{13}C-NMR (500 MHz) in $CDCl_3$ of **18**.

Target Compound Screening Report

Results Acquired by The University of Texas at Austin Mass Spectrometry Facility

Data File	MSF18-0611(BNB180)_hrESIpos1.d	**Sample Name**	0611(BNB180)	**Comment**	0611(BNB180)
Position	P1-A6	**Instrument Name**	Instrument 1	**User Name**	
Acq Method	pos.m	**Acquired Time**	4/25/2018 12:57:31 PM	**DA Method**	KS.m

MS Zoomed Spectrum

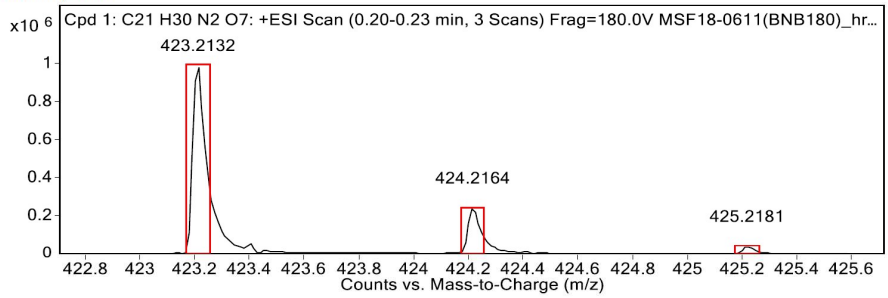

MS Spectrum Peak List

Obs. m/z	Calc. m/z	Charge	Abundance	Formula	Ion Species	Tgt Mass Error (ppm)
323.1610			1068477			
423.2132	423.2126	1	988952	C21H30N2O7	(M+H)+	-1.5
424.2164	424.2158	1	243363	C21H30N2O7	(M+H)+	-1.32
425.2181	425.2183	1	42354	C21H30N2O7	(M+H)+	0.3
426.2222	426.2208	1	5211	C21H30N2O7	(M+H)+	-3.2
427.2179	427.2233	1	1299	C21H30N2O7	(M+H)+	12.77

--- End Of Report ---

Figure 4.29: High Resolution Mass Spectrum (ESI positive mode) of **18**.

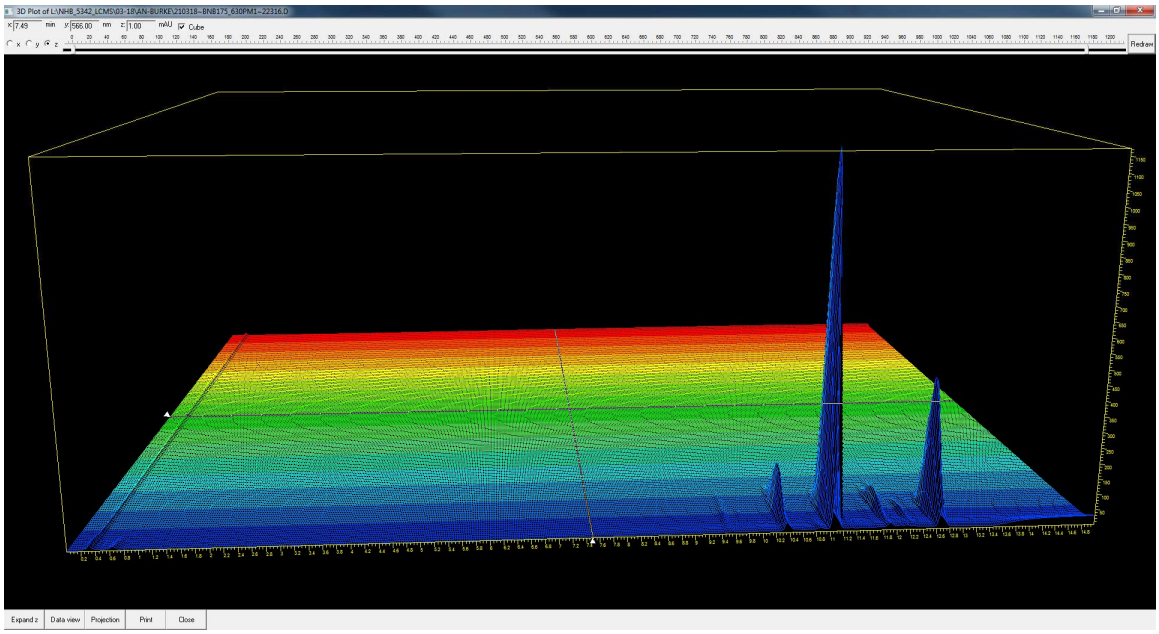

Figure 4.30: 3D LC trace of Claisen Reaction of **15**.

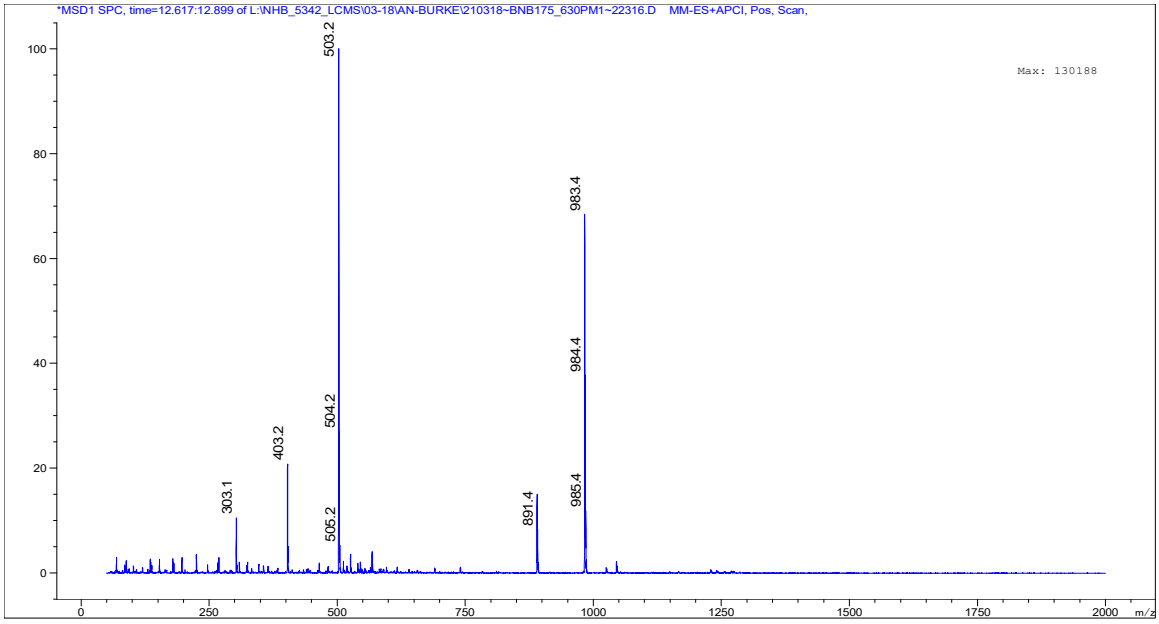

Figure 4.31: ESI/APCI positive ionization mass spectrum from 12.6 to 12.9 of **15**. $[M+Na]^+$ expected 503. $[2M+Na]^+$ expected 983.

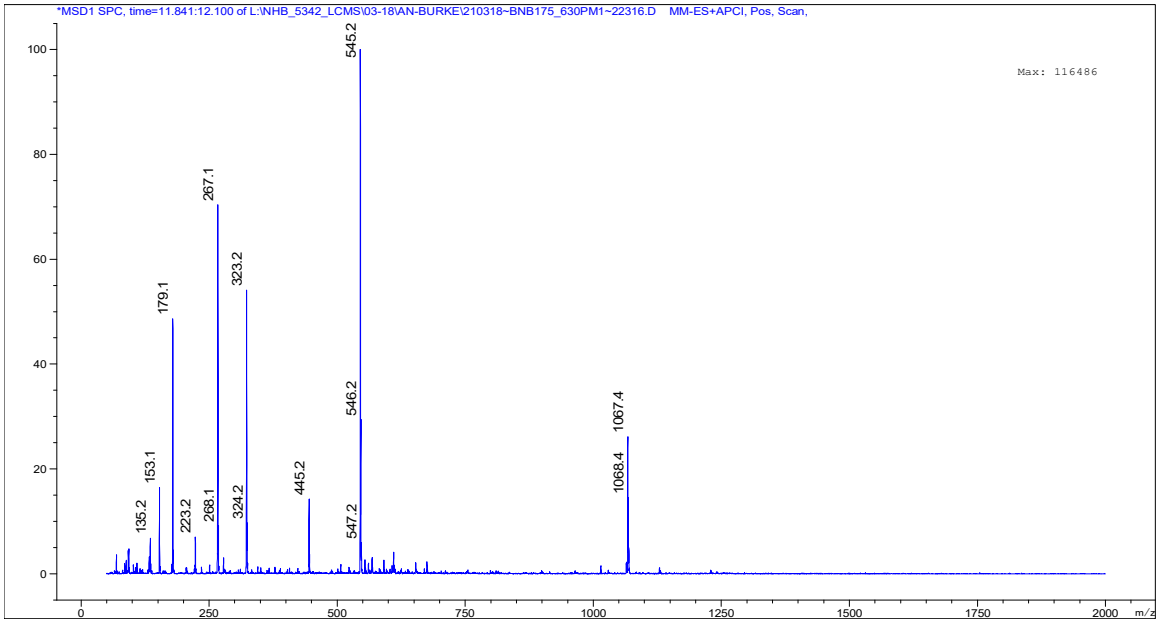

Figure 4.32: ESI/APCI positive ionization mass spectrum from 11.8 to 12.1 of **16**. $[M+Na]^+$ expected 545. $[2M+Na]^+$ expected 1067.

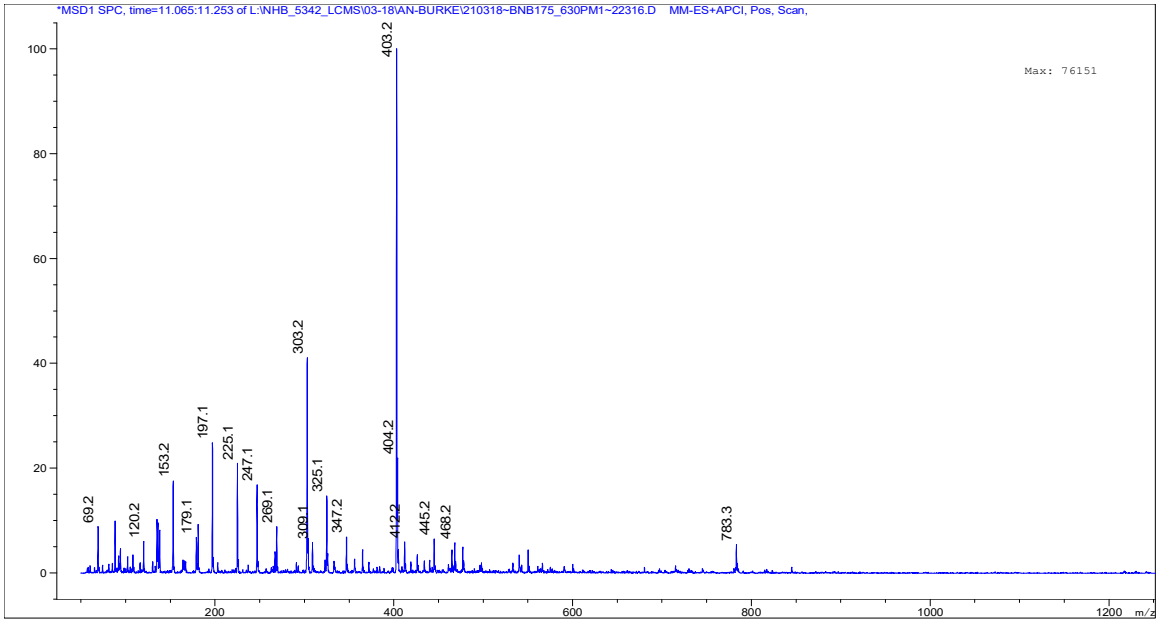

Figure 4.33: ESI/APCI positive ionization mass spectrum from 11.0 to 11.3 of **17**. $[M+Na]^+$ expected 403. $[2M+Na]^+$ expected 783.

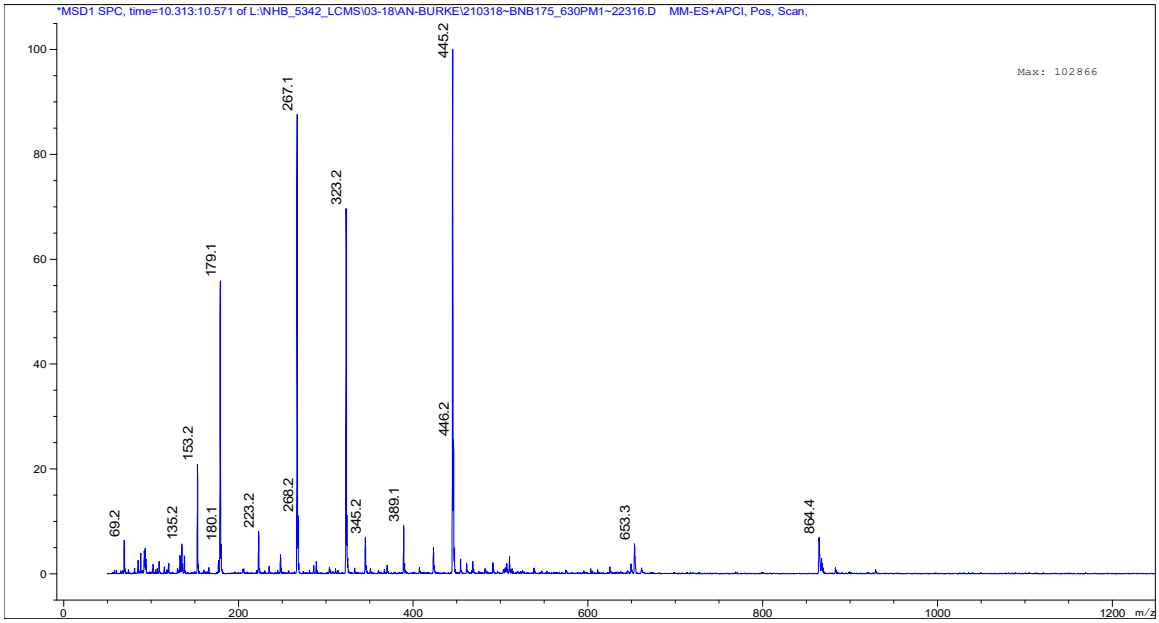

Figure 4.34: ESI/APCI positive ionization mass spectrum from 10.3 to 10.5 of **18**. $[M+Na]^+$ expected 445.

4.3.2.4 Boc Deprotection (M6)

Due to the rapid decomposition of **M6**, a wide range of deprotection solutions were screened with varying temperatures and time scales characterized by LC/MS and injectable mass spec, where **18**, mono-Boc, and **M6** were all observed, as well as a major decomposition product. The following procedures were screened:

20% TFA/DCM, RT, 24 hours, rotovapped

20% TFA/DCM, RT, 3 hours, N_2 blow dried

5% TFA/DCM, RT, 2 hours, quenched with HCl

TFA, RT, 1.5 hours

95% TFA/2.5% TIPS/2.5% H_2O, 0˚C, 1 hour, N_2 blow dried

95% TFA/2.5% TIPS/2.5% H_2O precooled to 0˚C, run at 0˚C, 1 hour, N_2 blow dried

1.25M Hydrogen Chloride in EtOH, RT, 5 hours, N_2 blow dried

2M Hydrogen Chloride in Et_2O, RT, 5 hours, N_2 blow dried

TFA-D, RT, 1 hour (NMR test)

87.5% TFA/2.5% TIPS/10% dry EtOH, -5˚C, 1 hour, N_2 blow dried

95% TFA/2.5% Tips/2.5% H_2O precooled to -5˚C, run at -5˚C, 3 hours, N_2 blow dried while remaining at -5˚C

The last of the reaction conditions was determined to provide the greatest amount of **M6** and minimized side product formation, so the reaction was scaled up. A solution of 95% TFA/2.5% triisopropylsilane/2.5% H_2O created and cooled to -5˚C. **18** (mmol, eq.) cooled to -5C, and dissolved in 5 mL TFA/TIPS solution. Reaction was monitored by LC/MS, and after 3 hours, a good amount of **M6** was observed, along with small amounts of **18** and side product. The solution was then blow dried with N_2(g) while still kept at -5˚C, being cautious to keep the solution as cool as possible. If solution splashed onto the side of the flask above the level of water bath, it would form a deep yellow solid, indicating

undesired side product formation. After an hour of gentle cooling, the small amount of solution was taken up in pre-cooled H_2O at 0˚C and injected onto the CombiFlash. Immediately as fractions came off the CombiFlash, the fraction was characterized by injectable mass spectrum, and frozen. After lyophilization, the product was taken up in 0.1M HCl, and characterized by injectable mass spectrum, and LC/MS. Characterization before lyophilization showed pure **M6**, however after lyophilization, a lot of a new side product was observed. By LC/MS, it is hypothesized that this new product was a dimer of the monomer (**Figure 4.35-4.37**). At this time, it was determined that if the monomer could not survive deprotected during the very mild condition of lyophilization, it would likely not survive the conditions required to load onto tRNA.

(**Figure 4.34**) HRMS-ESI $[M + Na]^+$ calculated for $C_{11}H_{14}N_2O_3$ 245.0897, found 245.0906.

Target Compound Screening Report

Results Acquired by The University of Texas at Austin Mass Spectrometry Facility

Data File	MSF18-0610(BNB183)_hrColESIpos3.d	**Sample Name**	0610(BNB183)	**Comment**	0610(BNB183)
Position	P1-A7	**Instrument Name**	Instrument 1	**User Name**	
Acq Method	New_pos_column_12min.m	**Acquired Time**	4/25/2018 4:10:56 PM	**DA Method**	LC_QTOF.m

MS Zoomed Spectrum

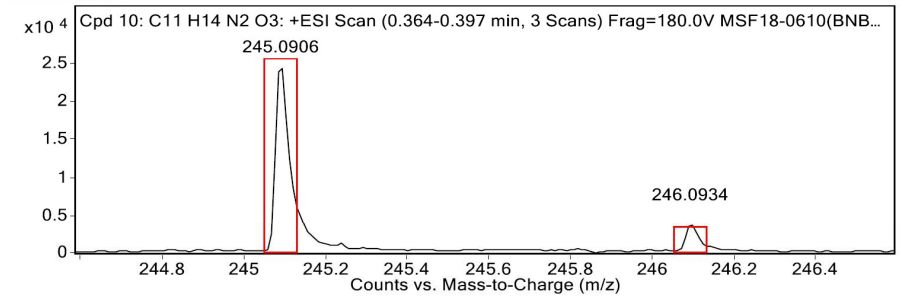

MS Spectrum Peak List

Obs. m/z	Calc. m/z	Charge	Abundance	Formula	Ion Species	Tgt Mass Error (ppm)
245.0906	245.0897	1	25033	C11H14N2O3	(M+Na)+	-3.63
246.0934	246.0927	1	3818	C11H14N2O3	(M+Na)+	-2.65
247.1077			285754			

--- End Of Report ---

Figure 4.35: High Resolution Mass Spectrum (ESI positive mode) of **M6**.

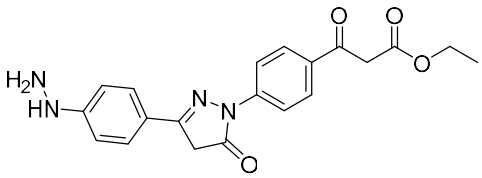

Figure 4.36: Hypothesized **M6** dimer moiety.

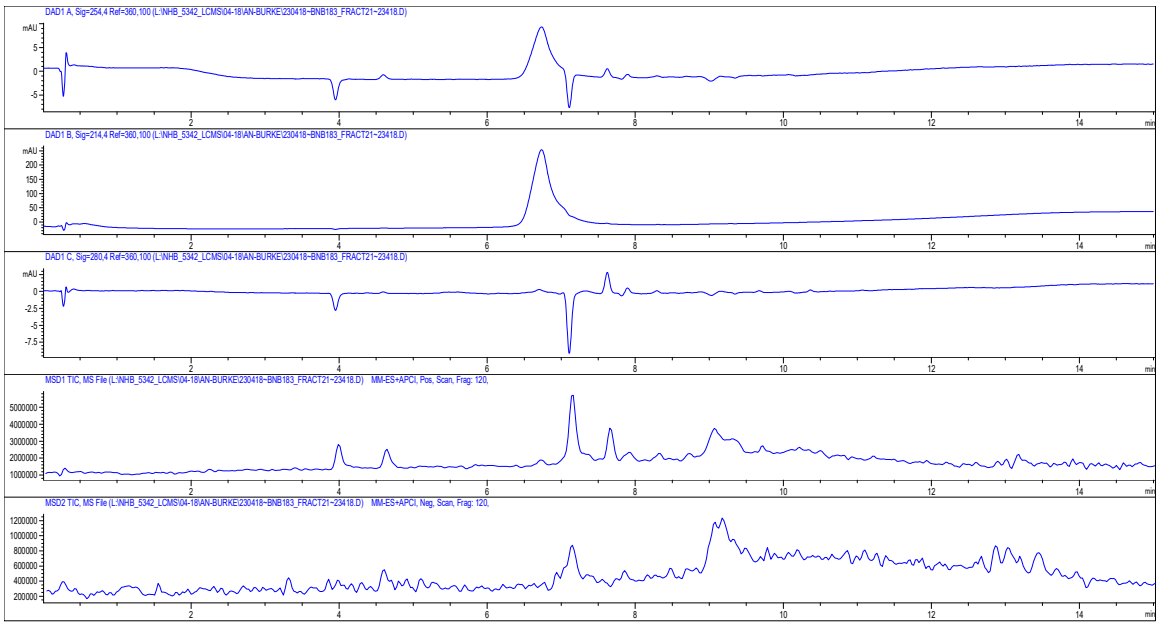

Figure 4.37: LC/MS data of **M6** and dimer after lyophilization. LC traces: at 254 nm, 214 nm, and 280 nm (frames 1-3). Mass detection: ESI/APCI positive ionization (frame 4), ESI/APCI negative ionization (frame 5).

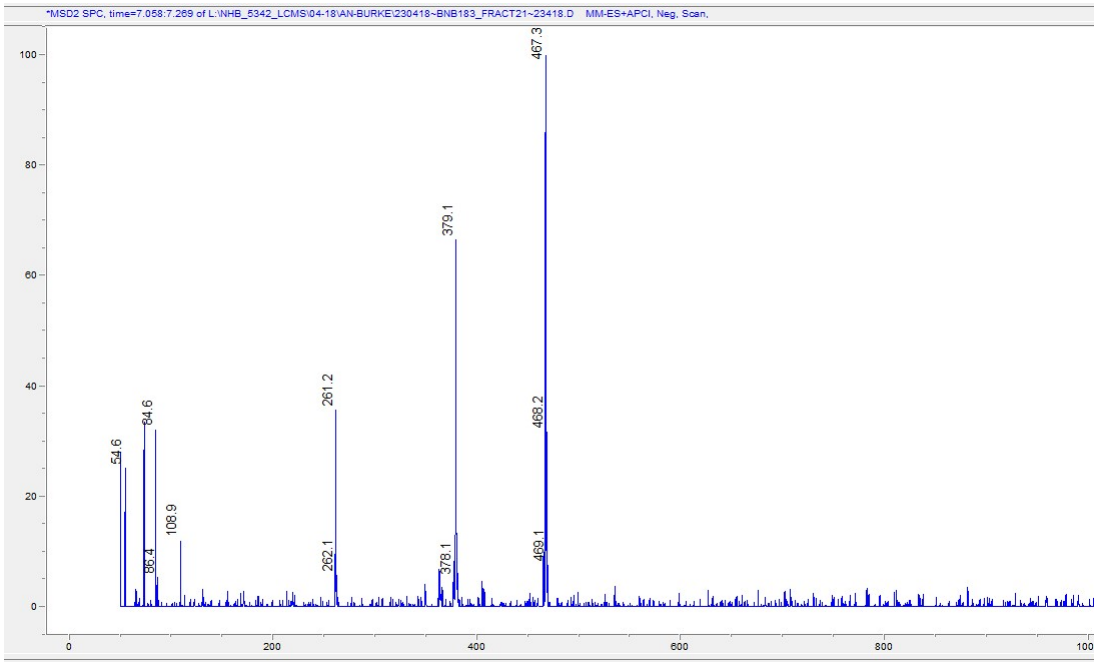

Figure 4.38: ESI/APCI negative ionization mass spectrum from 7.0 to 7.3 of **M6** dimer. $[M-H]^-$ expected 379.

Chapter 5: References for Part 1

(1) Fahnestock, S.; Rich, A. Ribosome-Catalyzed Polyester Formation. Science. **1971**, *173*(994), 340-343.

(2) Ohta, A.; Murakami, H.; Higashimura, E.; Suga, H. Synthesis of Polyester by means of Genetic Code Reprogramming. *Chem Biol*. **2007**, *14*(12), 1315-1322.

(3) Ohta, A.; Murakami, H.; Suga, H. Polymerization of alpha-Hydroxy Acids by Ribosomes. *Chembiochem*. **2008**, *9*(17), 2773-2778.

(4) Cox, M. M.; Doudna, J. A.; O'Donnell, M. Molecular Biology: Principles and Practice. **2012**, *5,* 615-659.

(5) Huang, L.; Dyer, R.; Lago, R.; Stolov, A.; Li, J. Mechanical Properties of Polyimide Coated Optical Fibers at Elevated Temperatures. Optical Fibers and Sensors for Medical Diagnostics and Treatment Applications. **2016**, *9702*, 97020Y-1 - 97020Y-8.

(6) Anslyn, E.; Dougherty, D. Modern Physical Organic Chemistry. **2006**, 568 - 569

(7) Kudirka, R.; Barfield, R.; McFarland, J.; Drake, P.; Carlson, A.; Banas, S.; Zmolek, W.; Garofalo, a.; Rabuka, D. Site-Specific Tandem Knoevenagel Condensation-Michael Addition to Generate Antibody-Drug Conjugates. *ACS Med. Chem. Lett*. **2016**, *7*(11), 994-998.

(8) Rostovski, N.; Ruvinskaya, J.; Novikov, M.; Khlebnikov, A.; Smetanin, I.; Agafonova. Switchable Synthesis of Pyrroles and Pyrazines via Rh(II)-Catalyzed Reaction of 1,2,3-Triazoles with Isoxazoles: Experimental and DFT Evidence for the 1,4-Diazahexatriene Intermediate. *J. Org. Chem*. **2017**, *82*(1), 256-268.

(9) Kuznetsova, V.; Davydov, A.; Vasiliskov, V.; Stomakhin, A.; Chudinov, A.; Zasedatelev. Novel Asymmetric IndodicarBOCyanine Dyes. *Russ. Chem. Bull., Int. Ed*. **2007**, *56*(11), 2263-2267.

(10) Bellamy, F.; Ou, K. Selective Reduction of Aromatic Nitro Compounds with Stannous Chloride in Non-Acidic and Non-Aqueous Medium. *Tet. Let*. **1984**, *25*(8), 839-842.

(11) Chandrappa, S.; Vinaya, K.; Ramakrishnappa, T.; Rangappa, K. An Efficient Method for Aryl Nitro Reduction and Cleavage of Azo Compounds Using Iron Powder/Calcium Chloride. *Synlett*. **2010**, *20*, 3019-3022.

(12) Alexander, M.; McDonald, J.; Ni, Y.; Niu, D.; Petter, R.; Qiao, L.; Singh, J.; Want, T.; Zhu, Z. MK2 Inhibitors and Uses Thereof. WO 2014/149164. **2014**.

(13) Kelly, M.; Kincaid, J.; Janagani, S.; Duncton, M. Amide Derivatives as Ion-Channel Ligands and Pharmaceutical Compositions and Methods of Using the Same. US 2006/0205773 A1. **2006**.

(14) Faul, M.; Oliver, T. Tin(II) Chloride. *E-EROS*. **2005**, 1-10.

(15) Gopinath, R.; Haque, J.; Patel, B. Tetrabutylammonium Tribromide (TBATB) as an Efficient Generator of HBr for an Efficient Chemoselective Reagent for Acetalization of Carbonyl Compounds. *J. Org. Chem*. **2002**, *67*(16), 5842-5845

(16) Ueno, A.; Kitawaki, T.; Chida, N. Total synthesis of (±)-Murrayazoline. *Org. Lett*. **2008**, *10*(10), 1999-2002.

(17) Loog, O.; Maeorg, U.; Ragnarsson, U. Synthesis of Hydrazines with Aromatic Substituents Using Triarylbismuth Reagents. *Synthesis*. **2000**, *11*, 1591-1597.

(18) Gut, J. Synthesis of Trimellitic and hemimellitic acids. *Chem. Listy*. **1956**, *21*, 1648-1650.

(19) Isoda, S.; Seiyaku, D. Medicinal Chemical Studies on Antiplasmin Drugs. VIII. 4-Aminomethylcyclohexanecarboxylic Acid Derivatives having a Carboxyl or Carboxymethyl Group at C_2. *Chem. Pharm. Bull*. **1980**, *28*(8), 2337-2346.

PART 2: PREPARATION FOR PDCPA CHARGING

Chapter 6: Introduction and Background

The ribosome has had millions of years of evolution to become a highly efficient catalyst for natural peptide bond formation. Not only does it have a high rate of polymerization at 20 amino acids per second, but it also has mechanisms to detect and prevent errors allowing for an accuracy of 99.99%.[1-2] Catalytic peptide bond formation is highly efficient due to amino acids placed only 7 Å apart in the active site, as well as water molecules located close to the active site, the peptidyl transferase center (PTC).[3-6] To capitalize on this efficiency, research has begun to discover a range of chemistries that could be carried out by a genetically modified ribosome.

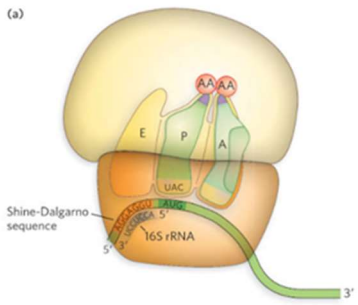

Figure 6.1: Ribosome with the small and large subunits, mRNA, tRNA, and the amino acids in the PTC site.[3]

There are three tRNA binding sites in the ribosome, the aminoacyl-tRNA site (A-site), the peptidyl-tRNA site (P-site), and the exit site (E-site). Translation is initiated when mRNA binds to the small ribosomal subunit, followed by incorporation of tRNA into the P-site, and finally the attachment of the large ribosomal subunit. Elongation of the peptide occurs by association and dissociation of various aminoacyl-tRNA species into the A-site

until the complementary anti-codon of the tRNA correctly matches the codon site of the mRNA. Once the correct tRNA has been associated, peptide bond formation is catalyzed in the PTC. Translocation occurs by shifting the tRNA in the P-site to the E-site, and the tRNA in the A-site into the P-site to both discard the used tRNA, and to vacate the A-site for new aminoacyl-tRNA association.

Once a monomer has been selected based on test chemistries and synthesized, it must then be charged onto tRNA to be shuttled into the ribosome for polymerization. One method for charging tRNA that is being investigated by the Moore group utilizes flexizyme chemistry to catalyze the charging of tRNA.[7] The mechanism of which is not completely understood, but it is hypothesized that the flexizyme works to increase the nucleophilicity of the tRNA.

Robertson, et al. have proposed another mechanism for charging non-natural amino acids onto tRNA by protecting the amine end with photo-labile NVOC, activating the ester by cyanomethylation, and charging the monomer onto a dinucleotide, pdCpA.[8-11] The charged pdCpA moiety is then ligated onto tRNA-CA, tRNA with its last two nucleotides, C and A, cleaved off (**Figure 8.1**). Both methods will be investigated to widen the pool of monomers loaded onto tRNA.

Chapter 7: Results and Discussion

7.1 NVOC-Cl Synthesis

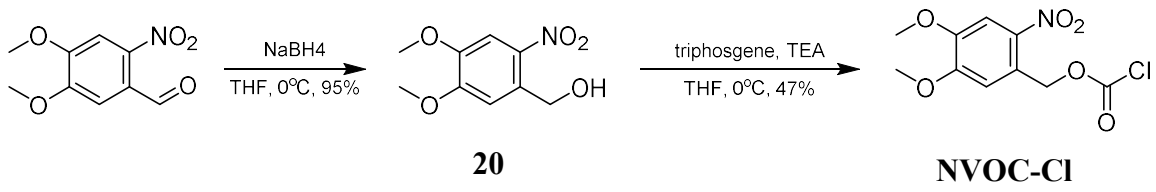

20 **NVOC-Cl**

Figure 7.1: NVOC-Cl synthesis.

Photo-labile protecting group NVOC-Cl is commercially available for $150/1g. Because a large amount of NVOC-Cl is required for the charging of pdCpA with different monomers, a synthetic route was followed by first reducing the aldehyde to **20**, followed by nucleophilic attack on triphosgene.[12-13] Recrystallization in toluene provided large amount of pure NVOC-Cl.

7.2 PDCPA SYNTHESIS

7.2.1 Schultz's Method

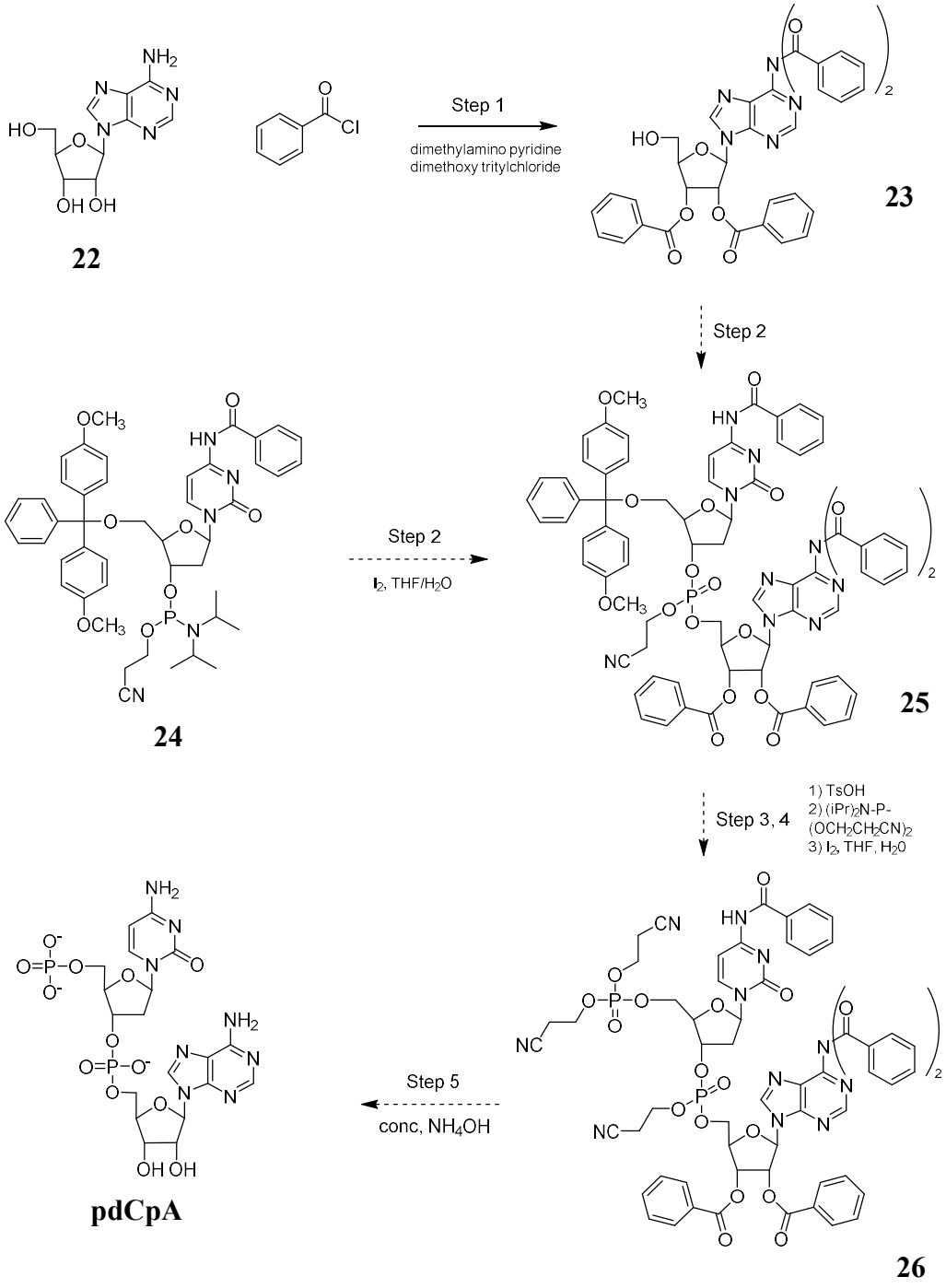

Figure 7.2: Schultz's manual synthesis.

Step 1 of the Schultz method involves trityl protection of the primary alcohol, benzoyl protection of the secondary alcohols and the primary amine, followed by cleavage of the trityl protecting group, and finally purification by column chromatography.[8-9,11] Upon characterization by LC/MS, **23** was identified, however, mono- di- and tri-benzoyl products were also observed in significant quantity. After attempted purification by column chromatography, only a very small amount of impure **23** was able to be isolated. Due to the difficulty in obtaining large amounts of pure product for first step, new methods of pdCpA synthesis were investigated.

7.2.2 Automated DNA Synthesizer

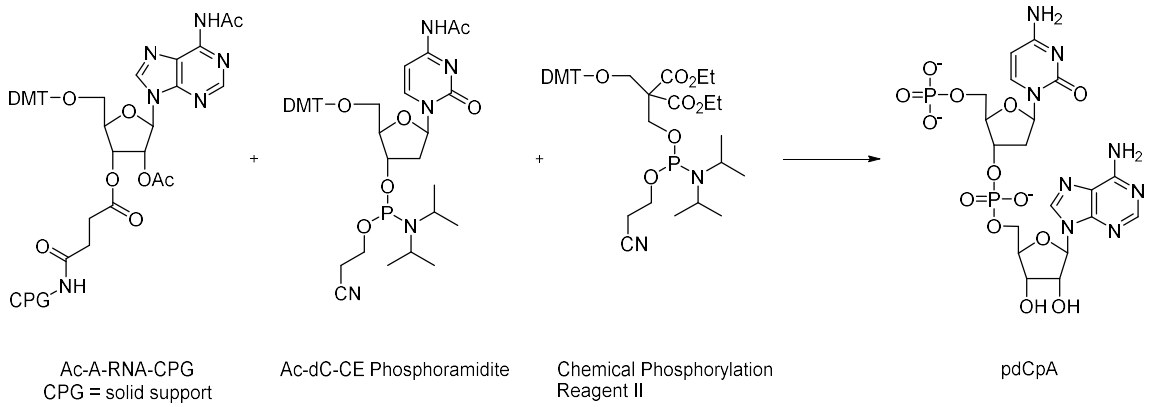

Figure 7.3: pdCpA synthesis by DNA Synthesizer.

The method of utilizing an ABI 8909 Expedite DNA Synthesizer to create pdCpA by solid phase synthesis was then investigated. Solid phase support, CPG, charged with the first nucleotide is purchased pre-loaded on a column, and synthesis from 3' to 5' is automatically performed on the synthesizer. After synthesis is complete, the protected DNA is cleaved from the resin, and loaded onto Glen-Pak Purification Cartridges for purification and deprotection of the remaining protecting groups. Although this synthesis

allowed for the synthesis of pure pdCpA, the maximum solid phase column size is one μmol. In order to load a series of different monomers onto pdCpA, a scale of mmol is required. Because it would take weeks of repetitive synthesis to compile those small scales into a useful scale, a new method for synthesis was devised modeling this protocol and materials as a base structure.

7.2.3 Manual DNA Synthesizer Method

In an attempt to scale up the amount of product produced without linearly scaling up the time, a manual synthesis protocol was devised and tested. Using a fritted column with a continuous flow of dry N_2(g), manual synthesis was able to be carried out on a larger scale using all of the same reagents that were used in the DNA synthesizer. A few alterations needed to be made to the protocol to get the synthesis to work. Firstly, the order of the oxidation and capping steps needed to be reversed to ensure proper oxidation of the phosphityl groups. Additionally, leaving the activating solution in the column when the phosphoramidite was added aided in coupling. Finally, deprotection of the acetyl groups was able to occur at the same time as cleavage from the column, eliminating the need to perform the tedious Glen-Pak purification. This synthesis provided a pure product in one day of synthesis, and one day of work-up. As more monomers are needed to be charged onto tRNA, this should provide a useful method in obtaining a relatively large scale of product in a short amount of time by simply increasing the scale of each of the reagents.

Chapter 8: Conclusions and Future Work

Once a monomer has been identified and synthesized, it will need to be charged onto tRNA. The monomer can be charged onto tRNA by flexizyme chemistry, investigated by the Moore group or by pdCpA following **Figure 8.1**. Both methods for charging tRNA will be investigated, as there have been some limitations on what can be charged utilizing the flexizyme chemistry, so using both techniques will hopefully widen the available library of monomers charged to tRNA.

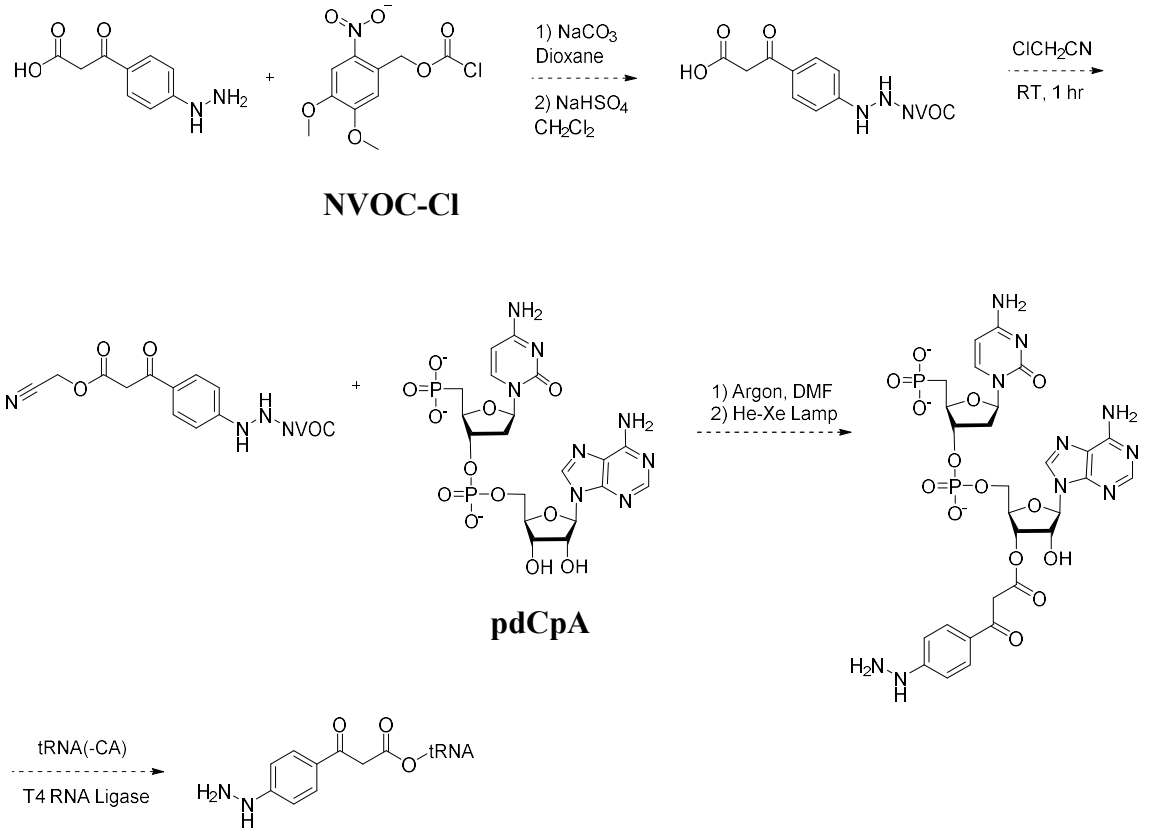

Figure 8.1: Scheme 7 monomer charging onto tRNA via pdCpA.

To load by pdCpA, the carboxylic monomer will have any amine or hydrazine groups protected by NVOC-Cl, followed by cyanomethylation, charging onto pdCpA, and

NVOC cleavage using a He-Xe lamp. Finally, the charged pdCpA will be ligated by T4 RNA Ligase to tRNA that has has the last two nucleotides, C and A, cleaved.

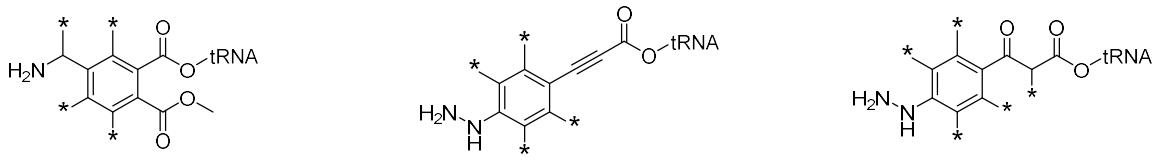

Figure 8.2: Scheme 3, 6, and 7 monomers with possible positions of variability (indicated by *).

After attachment to tRNA by either flexizyme chemistry or by pdCpA, the charged tRNA will be used to attempt polymerization inside a genetically modified ribosome. Once a monomer has been shown to polymerize in a genetically modified ribosome, methods to diversify monomers by placing unique groups on monomers will be investigated (**Figure 8.2**). Assignment of each unique group to a corresponding tRNA anti-codon will allow the creation of sequence defined polymers in a genetically modified ribosome.

Chapter 9: Experimental

9.1 Materials And Methods

All chemicals were of reagent grade and used as purchased without further purification. Automatic DNA synthesis performed on ABI 8909 Expedite DNA Synthesizer. Columns were ordered through Glen Research specifically for Expedite synthesizers. All reagents and solutions for pdCpA synthesis in the automatic and manual DNA Synthesizer methods were purchased from Glen Research and stored under argon in a desiccator, and in a fridge if required, to maintain anhydrous conditions.

LC/MS spectra were obtained on an Agilent Technologies 6120 Single Quadrupole LC/MS spectrometer which utilized a 5-95% MeOH/H_2O gradient over 12 minutes, with atmospheric-pressure chemical ionization in both positive and negative mode. H-NMR (400 MHz) were acquired with an Agilent 400 MHz.

9.2 NVOC-Cl Synthesis

Following protocol outlined by Tang, et al., 6-nitroveratraldehyde dissolved in 50 mL dry THF, and cooled to 0˚C.[12] Sodium borohydride added to solution and stirred overnight under argon, monitored by TLC (1:1 hexane:ethyl acetate). After disappearance of starting material, reaction quenched with 100 mL water while still under argon, then extracted with dichloromethane twice. Organics combined and concentrated under reduced pressure to produce pure **20** (2.042 g, 95.45% yield).

(**Figure 9.1**) 1H NMR (499 MHz, Chloroform-d) δ 7.76 (s, 1H), 7.01 (s, 1H), 5.74 (s, 2H), 4.00 (d, J = 18.2 Hz, 6H).

Following protocol outlined by Mattelaer, et al, a solution of triethylamine (9.56 mmol, 1.0 eq.) in 25.0 mL dry THF was added dropwise over 30 minutes to a stirred solution of triphosgene (9.56 mmol, 1.0 eq.) and **NVOC-Cl** (9.56 mmol, 1.0 eq.) in 40.0

mL dry THF cooled to 0˚C.[13] After the solution was stirred overnight at room temperature, the suspension was filtered through a column frit to remove any solid, then was concentrated under reduced pressure. The crude product was recrystallized in dry toluene under argon to produce a dark crystal, **NVOC-Cl** (1.2395 g, 47.02% yield), which was characterized by ^{1}H-NMR.

(**Figure 9.2**) 1H NMR (400 MHz, Chloroform-d) δ 7.71 (s, 1H), 7.17 (s, 1H), 5.01 – 4.93 (m, 2H), 4.01 (s, 3H), 3.96 (s, 3H), 2.60 (t, J = 6.5 Hz, 1H).

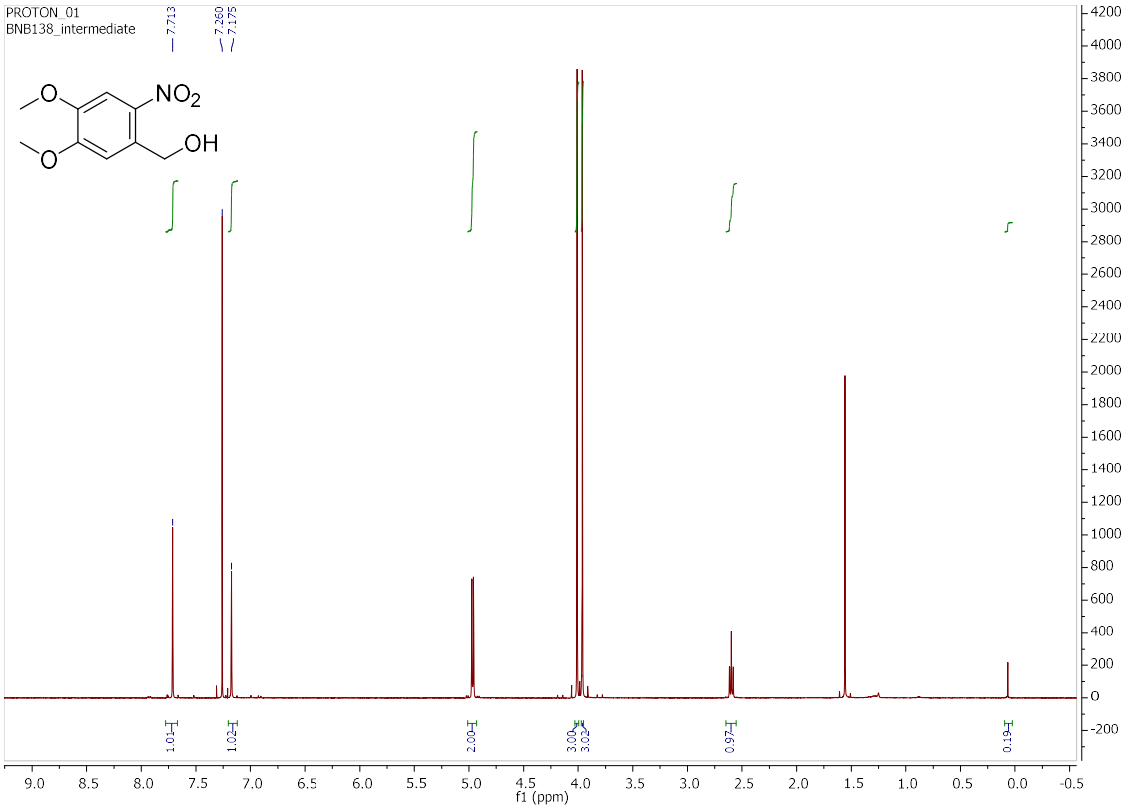

Figure 9.1: ^{1}H-NMR (400 MHz) $CDCl_3$ of **20**.

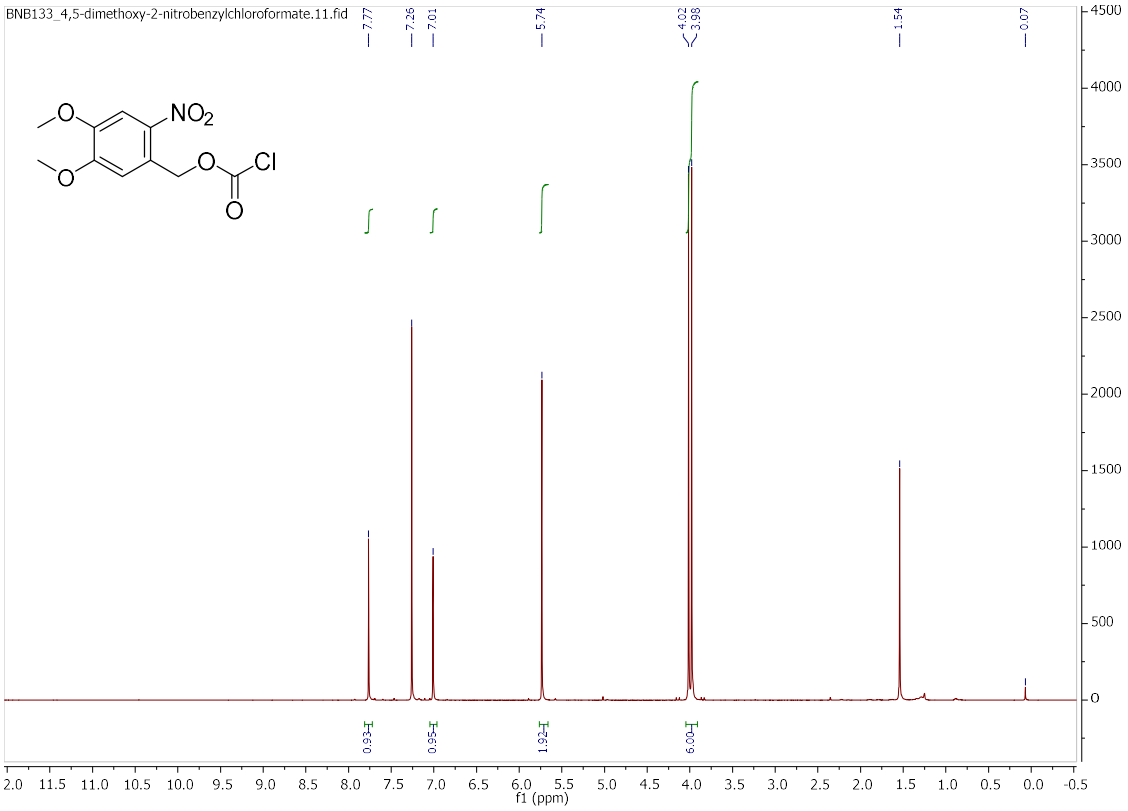

Figure 9.2: ^{1}H-NMR (400 MHz) $CDCl_3$ of **NVOC-Cl**.

9.3 pdCpA Synthesis

9.3.1 Automated DNA Synthesizer Method

Because the solid support can be purchased with one nucleotide already attached, the synthesis of pdCpA included only one nucleotide addition step and a phosphorylation coupling step. The cycle for solid phase synthesis on a DNA synthesizer goes through four steps per nucleotide addition: TCA deprotection of DMT, followed by coupling of phosphoramidite with tetrazole, then iodine oxidation of phosphityl groups, and finally capping of unreacted primary alcohols to prevent polymerization of uncoupled strands. The DNA strand is then cleaved from the resin using 1.0 mL ammonium hydroxide. The solution is loaded directly onto Glen-Pak cartridges, which attaches to the remaining DMT

group of any correctly synthesized strands. Following the protocol provided by Glen Research with the purchase of the Glen-Pak, a series of cleansing and cleavage solutions were pushed through the column and purified deprotected product was eluted with 0.5% ammonium hydroxide in 1 mL 50% acetonitrile in water. The compound was HPLC purified, and characterized by LC/MS.

9.3.2 Manual DNA Synthesizer Method

Anhydrous conditions must be maintained as best as possible, or this synthesis will not work. All solutions, including acetonitrile, were purchased from Glen Research, and stored under argon throughout synthesis. Manual solid phase synthesis was performed on a glass column cleaned with dichloromethane, hexanes, ethyl acetate, acetone, water, and plenty of (non-dry) acetonitrile, followed by at least 24 hours in an oven. The column was then plugged with a septum and purged with N_2(g) with a wide gauge needed that was first run through desiccant, into Schlenk line attached to the column, and an exit port through a silicone oil bubbler to maintain anhydrous conditions, prevent buildup of pressure, and to monitor flow rate of N_2. Throughout synthesis the flow of N_2 must be high enough to push solvent through the column when the valve is open, while simultaneously pushing through the bubbler. Manual shaking of column used to ensure distribution of solutions.

Directly before beginning synthesis, four solutions must be made fresh. 10 mL dry acetonitrile added to 0.5 g Ac-dC-CE Phosphoramidite to bring to a concentration of 0.067M. 5 mL dry acetonitrile added to 0.25 g Chemical Phosphorylation Reagent II to bring to a concentration of 0.067M. Capping mix was made by combining 5 mL Cap Mix A with 8 mL Cap Mix B. Finally, 1:1 (v:v) methylamine solution 40 wt.% in H_2O/ammonium hydroxide are combined to create an AMA solution.

Once the column and solutions were prepared, the CPG solid support (0.1 g CPG) was poured into the column, and acetonitrile was used to wash down the sides. Each coupling has four steps: deprotection, coupling, capping, and oxidation, with thorough dry acetonitrile washes after draining each step. Be sure to drain all of the liquid from the column on each step, to prevent reaction between reagents Deprotection solution (TCA) slowly added and drained continuously, while monitoring bright orange color indicating proper deprotection (approximately 12 mL was used). Once bright orange starts to fade in color on the column, the column was washed. Next, 0.9 mL tetrazole added and not drained, followed by addition of 2.0 mL of 0.067M Ac-dC-CE Phosphoramidite. The solution was incubated in the column for 30 minutes with occasional shaking, drained and washed. Next, 3.25 mL of the capping mixture added, and incubated for 5 minutes, drained and washed. 5 mL Iodine solution added to column, and incubated for 30 minutes with gentle shaking, drained and washed. After completion of the first coupling step, the same protocol will be followed for the second coupling step.

Deprotection solution (TCA) slowly added and drained continuously (approximately 10 mL was used), again looking for the bright orange appearance, then the column was washed. Next, 0.9 mL tetrazole added and not drained, followed by addition of 2.0 mL of 0.067M Chemical Phosphorylation Agent II. The solution was incubated in the column for 30 minutes with occasional shaking, then drained and washed. 3.25 mL of the capping mixture added, and incubated for 5 minutes, drained and washed. 5 mL Iodine solution added to column, and incubated for 30 minutes with gentle shaking, drained and washed.

Once both of the coupling steps have concluded, a final DMT deprotection step was performed by slow addition of deprotection solution (TCA) while draining continuously

(approximately 10 mL was used), again looking for the bright orange appearance one last time, then the column was washed.

At this point, the dinucleotide is still attached to the solid support with only acetyl protecting groups. Fortunately, both deprotection and cleavage from the resin are performed by incubating the column in 20 mL AMA overnight.

After collection of the liquid from the column, the solution was concentrated under reduced pressure using a Kolesnichenko contraption to produce pure **20**, characterized by HRMS.

(**Figure 9.3**) HRMS-ESI $[M + H]^+$ calculated for $C_{19}H_{26}N_8O_{13}P_2$ 637.1167, found 637.1152. (**Figure 9.4**) HRMS-ESI $[M - H]^-$ calculated for $C_{19}H_{26}N_8O_{13}P_2$ 635.1022, found 635.1040.

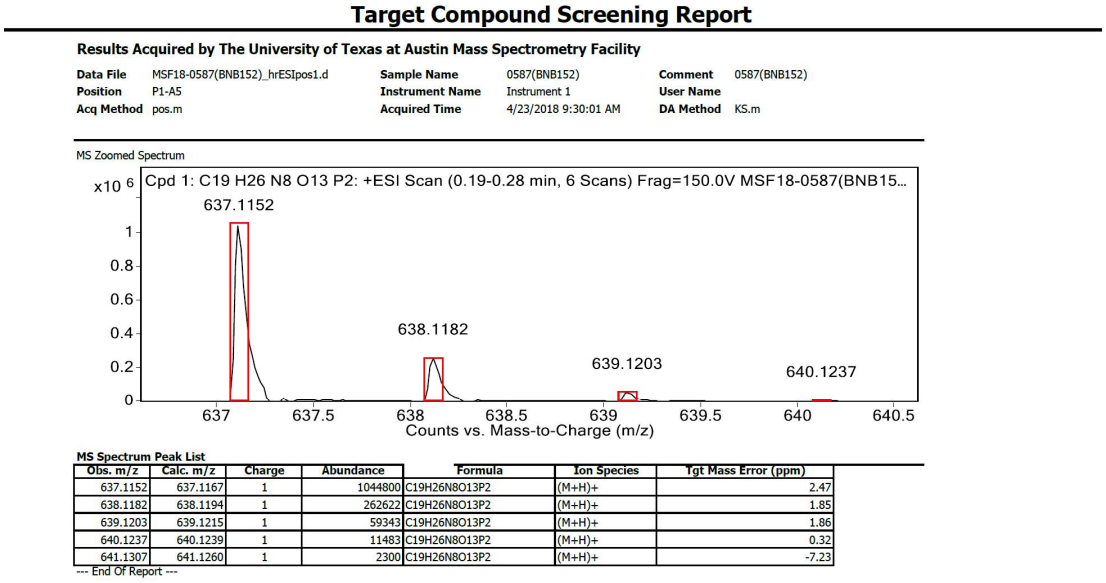

Target Compound Screening Report

Results Acquired by The University of Texas at Austin Mass Spectrometry Facility

Data File	MSF18-0587(BNB152)_hrESIpos1.d	**Sample Name**	0587(BNB152)	**Comment**	0587(BNB152)
Position	P1-A5	**Instrument Name**	Instrument 1	**User Name**	
Acq Method	pos.m	**Acquired Time**	4/23/2018 9:30:01 AM	**DA Method**	KS.m

MS Zoomed Spectrum

MS Spectrum Peak List

Obs. m/z	Calc. m/z	Charge	Abundance	Formula	Ion Species	Tgt Mass Error (ppm)
637.1152	637.1167	1	1044800	C19H26N8O13P2	(M+H)+	2.47
638.1182	638.1194	1	262622	C19H26N8O13P2	(M+H)+	1.85
639.1203	639.1215	1	59343	C19H26N8O13P2	(M+H)+	1.86
640.1237	640.1239	1	11483	C19H26N8O13P2	(M+H)+	0.32
641.1307	641.1260	1	2300	C19H26N8O13P2	(M+H)+	-7.23

--- End Of Report ---

Figure 9.3: High Resolution Mass Spectrum (ESI positive mode) of **20**.

Target Compound Screening Report

Results Acquired by The University of Texas at Austin Mass Spectrometry Facility

Data File	MSF18-0587(BNB152)_hrESIneg1.d	**Sample Name**	0587(BNB152)	**Comment**	0587(BNB152)
Position	P1-A5	**Instrument Name**	Instrument 1	**User Name**	
Acq Method	neg.m	**Acquired Time**	4/23/2018 9:33:06 AM	**DA Method**	KS.m

MS Zoomed Spectrum

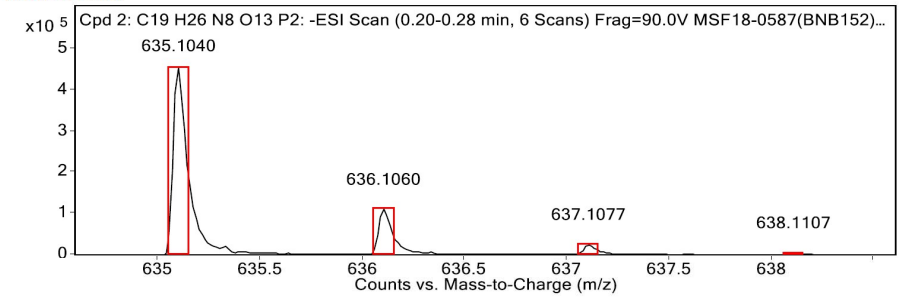

MS Spectrum Peak List

Obs. m/z	Calc. m/z	Charge	Abundance	Formula	Ion Species	Tgt Mass Error (ppm)
635.1040	635.1022	1	454471	C19H26N8O13P2	(M-H)-	-2.82
636.1060	636.1048	1	110287	C19H26N8O13P2	(M-H)-	-1.77
637.1077	637.1069	1	24859	C19H26N8O13P2	(M-H)-	-1.23
638.1107	638.1093	1	4664	C19H26N8O13P2	(M-H)-	-2.25
639.1187	639.1115	1	832	C19H26N8O13P2	(M-H)-	-11.33

--- End Of Report ---

Figure 9.4: High Resolution Mass Spectrum (ESI negative mode) of **20**.

Chapter 10: References for Part 2

(1) Bremer, H.; Dennis, P. Modulation of Chemical Composition and other Parameters of the Cell at Different Exponential Growth Rates. *EcoSal Plus*. **2008**, 1-49.

(2) Zaher, H.; Green, R. Fidelity at the Molecular Level: Lessons from Protein Synthesis. *Cell*. **2009**, *136*(4), 746-762.

(3) Cox, M. M.; Doudna, J. A.; O'Donnell, M. Molecular Biology: Principles and Practice. **2012**, *5,* 615-659.

(4) Sievers, A.; Beringer, M.; Rodnina, M.; Wolfenden, R. The Ribosome as an Entropy Trap. *Proc Natl Acad Sci U S A*. **2004**, *101*(21), 7897-7901.

(5) Rodnina, M.; Beringer, M.; Wintermeyer, W. How Ribosomes make Peptide Bonds. *Trends Biochem Sci*. **2007**, *32*(1), 20-26.

(6) Polikanov, Y.; Steitz, T.; Innis, C. A Proton Wire to Couple Aminoacyl-tRNA Accommodation and Peptide-Bond Formation on the Ribosome. *Nat Struct Molbio*. **2014**, *21*(9), 787-793.

(7) Ohuchi, M.; Murakami, H..; Suga, H. The Flexizyme System: a Highly Flexible tRNA Aminoacylation Tool for the Translation Apparatus. *Curr. Opin. Chem. Biol*. **2007**, *5*, 537-542.

(8) Robertson, S.; Noren, C.; Anthony-Cahill, S.; Griffith, M.; Schultz, P. The use of 5'-phospho-2 deoxyriBOCytidylylriboadensosine as a Facile Route to Chemical Aminoacylation of tRNA. *Nucleic Acids Res*. **1989**, *17*(23), 9649-9660.

(9) Robertson, S.; Ellman, J.; Schultz, P. A General and Efficient Route for Chemical Aminoacylation of Transfer RNAs. *J. Am. Chem. Soc*. **1991**, *113*(7), 2722-2729.

(10) Sinha, N.; Biernat, J.; McManus, J.; Koster, H. Polymer Support Oligonucleotide Synthesis XVIII: use of β-cyanomethyl-N,N-dialkylamino-/N-morpholino phosphoramidite of Deoxynucleosides for the Synthesis of DNA Fragments Simplifying Deprotection and Isolation of the Final Product. *Nucleic Acids Res*. **1984**, *12*(11), 4539-4557.

(11) Ellman, J.; Mendel, D.; Anthony-Cahill, S; Noren, C.; Schultz, P. Biosynthetic Method for Introducing Unnatural Amino Acids Site-Specifically into Proteins. *Methods in Enzymology*. **1991**, *202*, 301-336.

(12) Tang, S.; Wan, Z.; Gao, Y.; Zheng, J.; Wang, J.; Si, Y.; Chen, x.; Qi, H.; Liu, L.; Liu, W. Total Chemical Synthesis of Photoactivatable Proteins for Light-Controlled Manipulation of Antigen-Antibody Interactions. *Chem. Sci*. **2016**, *7*, 1891-1895.

(13) Mattelaer, H.; Mattelaer, C.; Papastavrou, N.; Dehaen, W.; Herdewijn, P. Oligonucleotide Promoted Peptide Bond Formation using a tRNA Mimicking Approach. *Chem. Commun*. **2017**, *53*, 5013-5016.

Bibliography

Fahnestock, S.; Rich, A. Ribosome-Catalyzed Polyester Formation. Science. **1971**, *173*(994), 340-343.

Ohta, A.; Murakami, H.; Higashimura, E.; Suga, H. Synthesis of Polyester by means of Genetic Code Reprogramming. *Chem Biol*. **2007**, *14*(12), 1315-1322.

Ohta, A.; Murakami, H.; Suga, H. Polymerization of alpha-Hydroxy Acids by Ribosomes. *Chembiochem*. **2008**, *9*(17), 2773-2778.

Cox, M. M.; Doudna, J. A.; O'Donnell, M. Molecular Biology: Principles and Practice. **2012**, *5,* 615-659.

Huang, L.; Dyer, R.; Lago, R.; Stolov, A.; Li, J. Mechanical Properties of Polyimide Coated Optical Fibers at Elevated Temperatures. Optical Fibers and Sensors for Medical Diagnostics and Treatment Applications. **2016**, *9702*, 97020Y-1 - 97020Y-8.

Anslyn, E.; Dougherty, D. Modern Physical Organic Chemistry. **2006**, 568 - 569

Kudirka, R.; Barfield, R.; McFarland, J.; Drake, P.; Carlson, A.; Banas, S.; Zmolek, W.; Garofalo, a.; Rabuka, D. Site-Specific Tandem Knoevenagel Condensation-Michael Addition to Generate Antibody-Drug Conjugates. *ACS Med. Chem. Lett*. **2016**, *7*(11), 994-998.

Rostovski, N.; Ruvinskaya, J.; Novikov, M.; Khlebnikov, A.; Smetanin, I.; Agafonova. Switchable Synthesis of Pyrroles and Pyrazines via Rh(II)-Catalyzed Reaction of 1,2,3-Triazoles with Isoxazoles: Experimental and DFT Evidence for the 1,4-Diazahexatriene Intermediate. *J. Org. Chem*. **2017**, *82*(1), 256-268.

Kuznetsova, V.; Davydov, A.; Vasiliskov, V.; Stomakhin, A.; Chudinov, A.; Zasedatelev. Novel Asymmetric IndodicarBOCyanine Dyes. *Russ. Chem. Bull., Int. Ed*. **2007**, *56*(11), 2263-2267.

Bellamy, F.; Ou, K. Selective Reduction of Aromatic Nitro Compounds with Stannous Chloride in Non-Acidic and Non-Aqueous Medium. *Tet. Let*. **1984**, *25*(8), 839-842.

Chandrappa, S.; Vinaya, K.; Ramakrishnappa, T.; Rangappa, K. An Efficient Method for Aryl Nitro Reduction and Cleavage of Azo Compounds Using Iron Powder/Calcium Chloride. *Synlett*. **2010**, *20*, 3019-3022.

Alexander, M.; McDonald, J.; Ni, Y.; Niu, D.; Petter, R.; Qiao, L.; Singh, J.; Want, T.; Zhu, Z. MK2 Inhibitors and Uses Thereof. WO 2014/149164. **2014**.

Kelly, M.; Kincaid, J.; Janagani, S.; Duncton, M. Amide Derivatives as Ion-Channel Ligands and Pharmaceutical Compositions and Methods of Using the Same. US 2006/0205773 A1. **2006**.

Faul, M.; Oliver, T. Tin(II) Chloride. *E-EROS*. **2005**, 1-10.

Gopinath, R.; Haque, J.; Patel, B. Tetrabutylammonium Tribromide (TBATB) as an Efficient Generator of HBr for an Efficient Chemoselective Reagent for Acetalization of Carbonyl Compounds. *J. Org. Chem*. **2002**, *67*(16), 5842-5845

Ueno, A.; Kitawaki, T.; Chida, N. Total synthesis of (±)-Murrayazoline. *Org. Lett*. **2008**, *10*(10), 1999-2002.

Loog, O.; Maeorg, U.; Ragnarsson, U. Synthesis of Hydrazines with Aromatic Substituents Using Triarylbismuth Reagents. *Synthesis*. **2000**, *11*, 1591-1597.

Gut, J. Synthesis of Trimellitic and hemimellitic acids. *Chem. Listy*. **1956**, *21*, 1648-1650.

Isoda, S.; Seiyaku, D. Medicinal Chemical Studies on Antiplasmin Drugs. VIII. 4-Aminomethylcyclohexanecarboxylic Acid Derivatives having a Carboxyl or Carboxymethyl Group at C_2. *Chem. Pharm. Bull*. **1980**, *28*(8), 2337-2346.

Bremer, H.; Dennis, P. Modulation of Chemical Composition and other Parameters of the Cell at Different Exponential Growth Rates. *EcoSal Plus*. **2008**, 1-49.

Zaher, H.; Green, R. Fidelity at the Molecular Level: Lessons from Protein Synthesis. *Cell*. **2009**, *136*(4), 746-762.

Cox, M. M.; Doudna, J. A.; O'Donnell, M. Molecular Biology: Principles and Practice. **2012**, *5,* 615-659.

Sievers, A.; Beringer, M.; Rodnina, M.; Wolfenden, R. The Ribosome as an Entropy Trap. *Proc Natl Acad Sci U S A*. **2004**, *101*(21), 7897-7901.

Rodnina, M.; Beringer, M.; Wintermeyer, W. How Ribosomes make Peptide Bonds. *Trends Biochem Sci*. **2007**, *32*(1), 20-26.

Polikanov, Y.; Steitz, T.; Innis, C. A Proton Wire to Couple Aminoacyl-tRNA Accommodation and Peptide-Bond Formation on the Ribosome. *Nat Struct Molbio*. **2014**, *21*(9), 787-793.

Ohuchi, M.; Murakami, H..; Suga, H. The Flexizyme System: a Highly Flexible tRNA Aminoacylation Tool for the Translation Apparatus. *Curr. Opin. Chem. Biol*. **2007**, *5*, 537-542.

Robertson, S.; Noren, C.; Anthony-Cahill, S.; Griffith, M.; Schultz, P. The use of 5'-phospho-2 deoxyriBOCytidylylriboadensosine as a Facile Route to Chemical Aminoacylation of tRNA. *Nucleic Acids Res*. **1989**, *17*(23), 9649-9660.

Robertson, S.; Ellman, J.; Schultz, P. A General and Efficient Route for Chemical Aminoacylation of Transfer RNAs. *J. Am. Chem. Soc*. **1991**, *113*(7), 2722-2729.

Sinha, N.; Biernat, J.; McManus, J.; Koster, H. Polymer Support Oligonucleotide Synthesis XVIII: use of β-cyanomethyl-N,N-dialkylamino-/N-morpholino phosphoramidite of Deoxynucleosides for the Synthesis of DNA Fragments Simplifying Deprotection and Isolation of the Final Product. *Nucleic Acids Res*. **1984**, *12*(11), 4539-4557.

Ellman, J.; Mendel, D.; Anthony-Cahill, S; Noren, C.; Schultz, P. Biosynthetic Method for Introducing Unnatural Amino Acids Site-Specifically into Proteins. *Methods in Enzymology*. **1991**, *202*, 301-336.

Tang, S.; Wan, Z.; Gao, Y.; Zheng, J.; Wang, J.; Si, Y.; Chen, x.; Qi, H.; Liu, L.; Liu, W. Total Chemical Synthesis of Photoactivatable Proteins for Light-Controlled Manipulation of Antigen-Antibody Interactions. *Chem. Sci*. **2016**, *7*, 1891-1895.

Mattelaer, H.; Mattelaer, C.; Papastavrou, N.; Dehaen, W.; Herdewijn, P. Oligonucleotide Promoted Peptide Bond Formation using a tRNA Mimicking Approach. *Chem. Commun*. **2017**, *53*, 5013-5016.

Bonnet, D.; Grandjean, C.; Rousselot-Pailley, P.; Joly, P.; Bourel-Bonnet, L.; Santraine, V.; Gras-Masse, H.; Melnyk, O. Solid-Phase Functionalization of Peptides by an α-Hydrazinoacetyl *Group. J. Org. Chem*. **2003**, *68* (18), 7033-7040.

Kozlecki, T.; Samyn, C.; Alder, R.; Green, P. Unexpected reactions of α,β-unsaturated esters with hydrazine hydrate. *J. Chem. Soc. Perkin Trans*. *2*. **2001**, *0*, 243-246.

Zixing, W.; Hedan, W.; Bowen, s.; Zhen, z.; Xiaoyu, Z.; Huibin, W. Heterocyclylpyri(mi)dinylpyrazole as Fungicidals. CN106883228, **2017**.

Deangelis A.; Wang, D.; Buchwald, S. Mild and Rapid Pd-Catalyzed Cross-Coupling with Hydrazine in Continuous Flow: Application to the Synthesis of Functionalized Heterocycles. *Angew. Chem. Int. Ed.* **2013**, *52* (12) 3434-3437.

Vogel, A. A Text Book of Practical Organic Chemistry, ELBS, Longman Group Ltd., **1975**, *3*, 594-611.

Bandgar, B.; Uppalla, L. Novel Chemoselective Reduction of Aryldiazonium Fluoroborates with Zn-$NiCl_2 \cdot 6H_2O$-THF. *J. Chem. Research*. **1999**, *0*, 714-715.

Deng, W.; Chen, D.;, Zhou, Y. Bicyclic Heterocyclies: Preparation and Pharmaceutical Applications. WO 2006/101456. **2006**.

Mojtahedi, M.; Niknejad, N.; Veisis, H. A Mild and Green Methos for the N-BOC Protection of Amines without Assistant of Catalyst Under Solvent-Free Conditions. *Letters in Organic Chemistry*. **2013**, *10*(2), 121-151

Raju, M.; Maeorg, S.; Tsubrik, O.; Maeorg, U. Efficient Solventless Technique for BOC-Protection of Hydrazines and Amines. *ARKIVOC*. **2009**, *6*, 291-297.

Frank, R.; Schutkowski, M. Extremely Mild Reagent for BOC Deprotection Applicable to the Synthesis of Peptides with Thioamide Linkages. *Chem. Commun*. **1996**, *0*, 2509-2510.

White, H. Manual Oligonucleotide Synthesis Using the Phosphoramidite Method. New Nucleic Acid Techniques. *Methods in Molecular Biology*. **1988**, *4*, 193-213

Janczyk, M.; Appel, B.; Springstubbe, D.; Fritz, H.; Müller, S. A New and Convenient Approach for the Preparation of β-Cyanoethyl Protected Trinucleotide Phosphoramidites. *Org. Biomol. Chem*. **2012**, *10*, 1510-1513.